



1 **Intercomparison of detection and quantification methods for methane emissions from**
2 **the natural gas distribution network in Hamburg, Germany**

3
4 Hossein Maazallahi^{1,2}, Antonio Delre³, Charlotte Scheutz³, Anders M. Fredenslund³, Stefan
5 Schwietzke⁴, Hugo Denier van der Gon², Thomas Röckmann¹

6
7 ¹*Institute for Marine and Atmospheric research Utrecht (IMAU), Utrecht University (UU),*
8 *Utrecht, The Netherlands*

9 ²*Netherlands Organisation for Applied Scientific Research (TNO), Utrecht, the Netherlands*

10 ³*Department of Environmental Engineering, Technical University of Denmark (DTU),*
11 *Lynby, Denmark*

12 ⁴*Environmental Defense Fund (EDF), Berlin, Germany*

13

14 **Correspondence:** Hossein Maazallahi (h.maazallahi@uu.nl)

15

16 **Abstract:**

17 In August and September 2020, three different measurement methods for quantifying methane
18 (CH₄) emission from leaks in urban gas distribution networks were applied and compared in
19 Hamburg, Germany: the “mobile”, “tracer release” and “suction” methods.
20 The mobile and tracer release methods determine emission rates to the atmosphere from
21 measurements of CH₄ mole fractions in the ambient air, and the tracer release method also
22 includes measurement of a gaseous tracer. The suction method determines emission rates by
23 pumping air out of the ground using soil probes that are placed above the suspected leak
24 location. The quantitative intercomparison of the emission rates from the three methods at a
25 small number of locations is challenging because of limitations of the different methods at
26 different types of leak locations.

27 The mobile method was designed to rapidly quantify the average or total emission rate of many
28 gas leaks in a city, but it yields a large emission rate uncertainty for individual leak locations.
29 Emission rates determined for individual leak locations with the tracer release technique are
30 more precise because the simultaneous measurement of the tracer released at a known rate at
31 the emission source eliminates many of the uncertainties encountered with the mobile method.
32 Nevertheless, care must be taken to properly collocate the tracer release and the leak emission
33 points to avoid biases in emission rate estimates. The suction method could not be completed
34 or applied at locations with widespread subsurface CH₄ accumulation, or due to safety
35 measures, and this sampling bias may be associated with a bias towards leak locations with low
36 emission rates. The leak locations where the suction method could not be applied were the
37 biggest emitters as confirmed by the emission rate quantifications using mobile and tracer
38 methods and an engineering method based on leak’s diameter, pipeline overpressure and depth
39 at which the pipeline is buried. The corresponding sampling bias for the suction technique led
40 to a low bias in derived emission rates in this study. It is important that future studies using the
41 suction method account for any leaks not quantifiable with this method in order to avoid biases,
42 especially when used to inform emission inventories.

43

44

45

46

47



1 Introduction

48
49
50
51
52
53
54
55
56
57
58
59
60
61
62
63
64
65
66
67
68
69
70
71
72
73
74
75
76
77
78
79
80
81
82
83
84
85
86
87
88
89
90
91
92
93
94
95
96

Natural gas combustion has a lower carbon footprint than combustion of other fossil fuel sources for the same thermal output (EIA, 2021). However, fugitive methane (CH₄) emissions can significantly turn the balance in terms of climate impact (Alvarez et al., 2012) because the global warming potential of CH₄ over a 20-year time scale is 84 times higher than that of carbon dioxide (CO₂) (Myhre et al., 2013). The atmospheric abundance of CH₄ has increased about 2.5-fold since the pre-industrial era (Bousquet et al., 2006). Following a short period of stable levels after the year 2000, atmospheric CH₄ has continued to increase since 2006. Worden et al (2017) concluded that about 50 to 80% of the post-2006 increase originated from fossil sources and Jackson et al. (2020) attributed the accelerated increase of 6 – 13 ppb yr⁻¹ from 2014 to 2017 (Nisbet et al., 2019), equally to the emission increase from fossil and agriculture sectors.

Gas distribution networks in cities are subject to maintenance programs by the operators to detect and fix leakages that occur, as CH₄ is an incendiary gas and can be explosive at concentrations between 4 and 16% in ambient air (DVGW, 2022). Since the safe operation of the distribution network and leak repair is the primary objective of this maintenance, quantification of emissions from leakages is rarely performed. The absence of regulations on CH₄ emissions is another reason why leak rates are not routinely quantified, however CH₄ emissions from the energy sector needs to be addressed properly within the EU CH₄ strategy by 2050 (EC, 2020). Nevertheless, from the perspective of climate change and possible mitigation options, it is important that emissions from gas leakages are (i) quickly detected and fixed and (ii) well quantified. Weller et al. (2020) and Alvarez et al. (2018) respectively reported 5 and 1.6 times higher CH₄ emissions from leaks in the US gas distribution network based on such observations compared to the national inventory reports.

Leaks from buried pipelines can be due to corrosion or failure/defects in joints or materials (EPA, 1996). When a leak occurs on a buried urban gas pipeline, the gas will generally accumulate in the air space below the surface and then find its path to the atmosphere through a single or several surface outlets. The outlets can be either unpaved soil surfaces, cracks in the road or pavements, or associated with different types of cavities (manholes, communication covers, rain drains, etc.). The major outlet is generally the one with the highest overall permeability for gas released from the buried natural gas pipeline. On the way from the leak location on a buried pipeline to the atmosphere through outlets, CH₄ may be oxidized by methanotrophs in the soil and/or merge with CH₄ from other sources, e.g. biogenic CH₄ emissions from sewage system.

Routine leak surveys in Germany are conducted by walking with handheld CH₄ sensors above buried pipelines, referred to as the carpet method (DVGW, 2019). The success of leak detection with the carpet method depends primarily on soil permeability (Ulrich et al., 2019), which is influenced by soil moisture, texture, soil organic content and the location of the groundwater table (Wiesner et al., 2016). Based on risk of explosion, gas leaks are classified into four types: A1, A2, B and C (DVGW, 2019). This classification is based on the accumulation of CH₄ in cavities (e.g. manholes, rain drains, etc.) or buildings and the distance of gas leaks to buildings and cavities. If natural gas leaks into buildings or cavities, the leak classifies as A1, and it must be repaired immediately to minimize explosion risk. If the gas leak has a distance up to 1 m to buildings and does not fill cavities, it is classified as A2, and it must be fixed within a week. If the distance is between 1 to 4 m to buildings, the leak is classified as B and the repair time



97 window is three months, and if the distance is more than 4 m then, the leak is considered as C
98 category and can be fixed according to the scheduled repair plan. Gas pipelines in a city with
99 the scale of Hamburg are monitored every 5 years with the carpet method. The leak emission
100 rate is not quantified and thus also not a parameter affecting the course of action.
101

102 In recent years, mobile measurement methods using vehicles with fast and high-precision laser
103 instrumentation have been established for leak detection and emission quantification in
104 numerous cities (Fernandez et al., 2022; Defratyka et al., 2021; Luetschwager et al., 2021;
105 Keyes et al., 2020; Maazallahi et al., 2020; Ars et al., 2020; Weller et al., 2018; von Fischer et
106 al., 2017; Jackson et al., 2014). In-situ measurements of atmospheric CH₄ from mobile vehicles
107 are used to pinpoint and quantify CH₄ emission sources at street level in urban areas. The
108 mobile method was calibrated using above-ground controlled release experiments, in which
109 known amounts of CH₄ were released from gas cylinders (Weller et al., 2019). Simultaneous
110 measurements of carbon dioxide (CO₂) and ethane (C₂H₆) can provide valuable additional
111 information for attributing CH₄ sources (Maazallahi et al., 2020). A characteristic of the
112 resulting emissions distribution from gas distribution grids in cities is the existence of a few
113 leak locations with very high leak rates, up to 100 L min⁻¹, resulting in a right-skewed leak
114 emission rate distribution (Weller et al., 2020). Usually about 10% of the leaks are responsible
115 for between 30% to 70% of the emissions (Weller et al., 2019; Maazallahi et al., 2020).
116 Therefore, the CH₄ emission from the gas distribution system can be reduced very effectively
117 if the largest leaks can be found and fixed quickly, thus augmenting the routine leak detection
118 (carpet method) and repair programs with the mobile method.
119

120 The tracer dispersion method is another method to quantify CH₄ emissions from point and area
121 sources. In this method, a tracer gas is released at a known rate close to the outlet of the gas
122 leak, and both tracer and target gas concentrations are measured downwind. From these
123 measurements and the known tracer gas release rate, the target gas emission rate can be
124 determined with an uncertainty of ± 15% (Lamb et al., 1995) or less than 20% (Fredenslund et
125 al., 2019). Lamb et al. (2015) applied the tracer method to quantify leaks from urban
126 underground pipelines where they reported moderate agreement (± 50%) to excellent
127 agreement (± 5%) between the tracer and high-flow sampler method.
128

129 Another approach to quantify underground leak rates from buried gas pipelines is the so-called
130 suction method. In this method air is pumped out of the ground at a known rate via probes
131 surrounding the underground leaks until an equilibrium CH₄ mixing ratio is reached in air out-
132 flow, from which the CH₄ leak rate can be calculated. In Germany, this approach is applied to
133 a limited number of leak locations, which do not have to be repaired immediately or within 1
134 week. Suction measurements normally find leak rates that are < 2 L min⁻¹ (E.ON, personal
135 communication, 2020). The reported uncertainty range of this method is ± 10% based on 23
136 measurements in the 1990s (E.ON, personal communication, 2020). The discrepancy between
137 these rather low leak rates compared to leak rates inferred with the mobile method calls for
138 further investigation, since the suction method is also employed to derive network-wide
139 emission factors for the German country-wide gas distribution network (Federal Environment
140 Agency, 2020).
141

142 Hendrick et al. (2016) used surface flux chamber measurements carried out between 2012 and
143 2014 to estimate gas leak rates from 100 leak locations in the Boston area that were detected
144 using mobile measurements (n = 45) in 2011 from Phillips et al. (2013) and additional locations
145 from later mobile surveys (n = 55). They reported CH₄ emission rates from gas leaks ranging
146 from 0.003 g min⁻¹ to 16 g min⁻¹, corresponding to roughly 0.0 – 24.4 L min⁻¹. They also



147 reported that their estimate using chamber measurements underestimated total CH₄ emissions,
148 likely because the chambers didn't capture the total CH₄ emitted from the leak. This is similar
149 to the enclosure measurements results from Weller et al. (2018).

150
151 The flow through a hole in a pipeline can also be calculated theoretically and empirically from
152 the physical properties of the hole, mainly the ratio of hole to pipeline diameter and the
153 overpressure in the pipeline. There are three different engineering model types to estimate
154 emissions from gas leaks: the hole model, the rupture model and modified models to bridge the
155 gap between hole and rupture models (Hu et al., 2020; Moloudi and Esfahani, 2014; Yuhua et
156 al., 2002; Arnaldos et al., 1998). These types of models are either to estimate leak strength from
157 a pipeline in open space or a buried pipeline. A leak on a buried pipeline has higher surrounding
158 resistance depending on soil conditions compared to a situation where the pipeline is in open
159 space. Such models have been used to quantify emissions from holes in pipelines in open space
160 (Hou et al., 2020; Manda and Morshed, 2017; Moloudi and Esfahani, 2014; Mahgerefteh, Oke
161 and Atti, 2005; Yuhua et al., 2003; Kayser and Shambaugh, 1991) but also from buried
162 pipelines (Liu et al., 2021; Ebrahimi-Moghadam et al., 2018; Okamoto and Gomi, 2011; Yan,
163 Dong and Li, 2015). Cho et al. (2021) introduced a model, which takes into account soil
164 properties including absolute and relative permeability and porosity, the underground spread
165 of the leak, surface CH₄ mole fractions and depth of the buried pipeline based on experiments
166 with a controlled release rate. This model was calibrated based on release rates ranging from
167 1.3 g min⁻¹ to 5.7 g min⁻¹, corresponding to roughly 2.0 – 8.7 L min⁻¹.

168
169 In this study, we present results from measurements with the mobile, the tracer release and the
170 suction methods in Hamburg, Germany, in August and September 2020. We present the
171 quantitative emission estimates as well as a qualitative intercomparison of the three methods,
172 in particular related to the applicability and the strengths and weaknesses of the different
173 methods at different leak locations. We investigate differences between the leaks detected from
174 mobile measurements and leak locations reported from the routine leak detection surveys
175 performed by the local gas utility (hereinafter LDC (Local Distribution Company)). Finally,
176 we discuss implications of our study for national emission inventories.

177

178 **2 Materials and Methods**

179 **2.1 Campaign preparation and general overview**

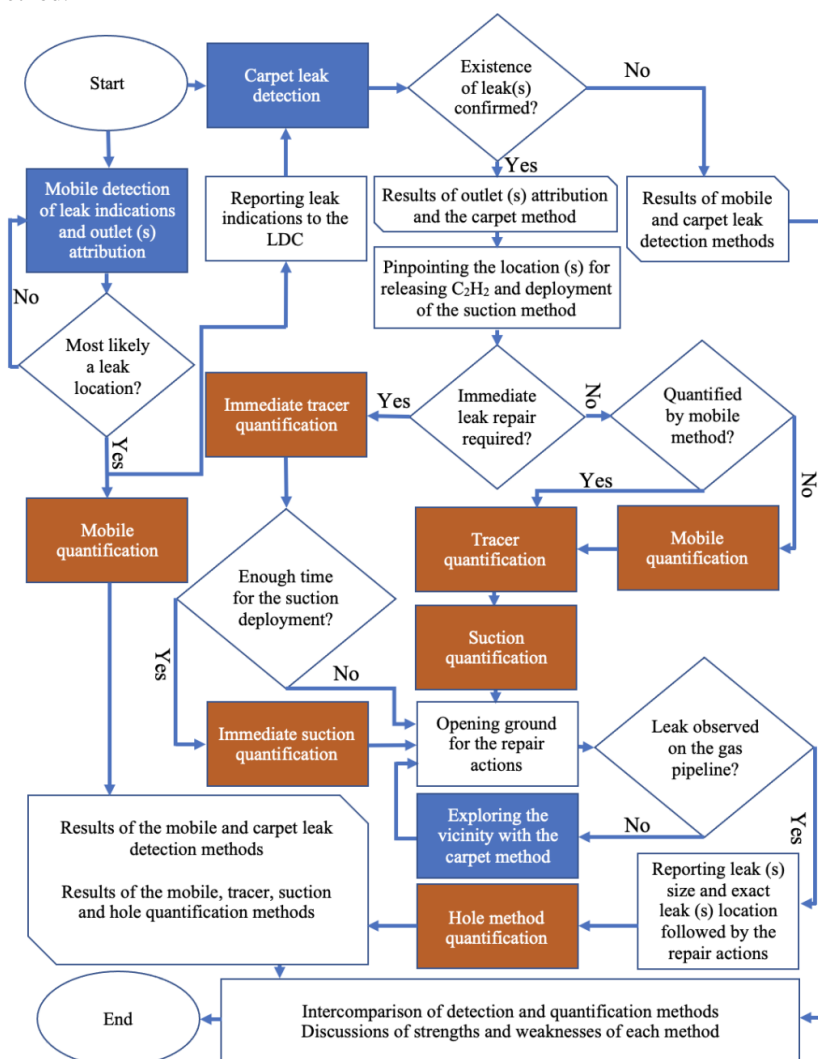
180 As a preparation for the intercomparison campaign, all partners contributed to the preparation
181 of an “intercomparison matrix” where the characteristics and deployment details of the
182 different methods were specified. This matrix is provided in section S.1 of the Supplemental
183 Information (SI). The matrix includes descriptions related to the identification of gas leaks, the
184 quantification of gas leaks, adjustments of the method to the intercomparison exercise and
185 upscaling. It also laid out an initial plan for the intercomparison in terms of identification of
186 suitable locations and deployment of the different methods.

187 According to this plan (Fig. 1), we first applied the mobile method to identify potential gas leak
188 locations, namely leak indications (LIs). When the mobile method had detected one or more
189 emission outlets (See Sect. S.2 in SI) and classified them as a potential gas leak location, the
190 carpet method was applied to confirm the leak and determine the confine leak location. Some
191 additional locations that had previously been identified by the carpet method (leak categories
192 B and C) were added to the list of target locations.

193 Following leak detection, the mobile quantification method (multiple transects) was applied on
194 all the locations and the tracer and suction methods were applied at the confirmed leak
195 locations, and with some restrictions regarding safety and method capacities. The release



196 location for the tracer quantification method was confirmed based on surface screening using
 197 a handled methane analyzer. For comparison of the mobile and tracer release methods with the
 198 suction and hole methods we assumed that (i) a steady state between pipeline leakage under-
 199 ground CH₄ accumulation and emission to the atmosphere had been reached (Kirchgeßner et
 200 al., 1997) and (ii) methanotrophs and methanogens have negligible impact on quantification of
 201 gas leak emissions. Thus, the total emission rate of all outlets in the vicinity of a leak location
 202 is equal to the natural gas emission rate from the pipeline leak. We will discuss implications of
 203 the above assumptions for selected cases. After leak repair, the LDC reported leak hole sizes,
 204 pipeline diameters and pipeline operational pressures, allowing leak rate estimation with the
 205 hole method.



206
 207 **Figure 1 – Flowchart of application of leak detection methods (blue colors) and**
 208 **quantification methods (red colors) followed by repair actions and intercomparison of**
 209 **the detection and quantification methods**
 210 **2.2 Measurements setups**



211 **2.2.1 Mobile measurement setup**

212 Onboard the measurement vehicle (VW Transporter) we operated two cavity ring-down
213 spectrometers (CRDS), model G2301 and model G4302 (Picarro, Santa Clara, California,
214 USA). The G2301 measures CH₄, CO₂ and water vapor (H₂O) at a flow rate of $\approx 0.2 \text{ L min}^{-1}$
215 and 0.3 Hz frequency. The G4302 has a flow rate of $\approx 2.2 \text{ L min}^{-1}$ and sampling frequency of
216 about 1 Hz for CH₄, C₂H₆ and H₂O. The air intake for both instruments was from the same
217 tubing attached to the front bumper. This setup allowed us to directly compare the
218 enhancements observed from the two instruments during surveys. The G4302, which is in a
219 shape of a backpack, was also used in attribution of outlets emissions in walking surveys to
220 check presence of C₂H₆ in emission outlets.

221

222 **2.2.2 Tracer release measurement setup**

223 The tracer release method was applied by releasing acetylene (C₂H₂) at the emission outlet
224 identified by the mobile leak detection and confirmed by the carpet method. The tracer gas
225 was released at the main emission outlet, which was confirmed by surface screening using a
226 handheld CH₄ analyzer. Tracer release rates between 1.3 and 2.6 L min⁻¹ from a gas cylinder.
227 A Picarro CRDS, G2203 instrument was used to measure CH₄ and C₂H₂ mole fractions
228 continuously with $\approx 0.3 \text{ Hz}$ frequency. The instrument was installed in a measurement vehicle
229 (VW Caddy), and air was sampled from the atmosphere through an inlet on the roof about 2m
230 above ground. The tracer method was applied either in static mode, where air was sampled in
231 one or a few locations downwind from the outlets and tracer release locations ($n = 11$) or mobile
232 mode ($n = 5$), where the plumes were transected while measuring concentrations of CH₄ and
233 C₂H₂. The choice of mode depended on the site conditions including road accessibility and
234 wind direction. The tracer release setup including instrumentation used as well as mobile mode
235 is described in detail in Mønster et al (2014), and the principle of the static mode is described
236 in Fredenslund et al (2010).

237

238 **2.2.3 Suction measurement setup**

239 In the suction method, 12 probes were used to insert in the soil around the confirmed gas leak
240 location by the LDC. The probes are connected to a pump to extract accumulated subsurface
241 CH₄ from the leak. CH₄ mole fraction at the outflow is measured with a Flame Ionization
242 Detector (GERG, 2018).

243

244 **2.2.4 Carpet method setup**

245 Leak detection experts from the LDC operate a methane detector (Sewerin instruments,
246 Gütersloh, Germany) on a rolling device, where a plastic cover (the carpet) moves over the
247 ground and provides a loose seal to the surrounding atmosphere, facilitating preferential
248 analysis of air emanating from the surface right below the carpet. The instrument gives an
249 acoustic signal when a high CH₄ from a potential leak has been detected. The instrument can
250 detect C₂H₆ with a gas chromatograph, which take about couple of minutes per outlet location.

251

252 **2.3 Detection, confirmation and attribution of emissions at gas leak locations**

253 **2.3.1 Mobile detection of possible leak location**

254 For leak detection with the mobile method, we first evaluated CH₄, C₂H₆ and CO₂ signals
255 during mobile surveys. If (i) CH₄ and C₂H₆ signals were observed with a ratio of less than 10%
256 with no CO₂ signal or (ii) CH₄ was observed ($< 500 \text{ ppb}$ enhancement on G4302) with no C₂H₆
257 and CO₂ signals, then we parked the mobile measurement car, detached the G4302 analyzer
258 from the system and searched for gas outlets on foot with the G4302. This detailed search for
259 outlets was performed to (i) confirm the presence of both CH₄ and C₂H₆ signals (ii) map the
260 spatial spread of outlets and (iii) spatially constrain the possible gas leak location. The reported



261 possible gas leak locations from the mobile method were then reported to the LDC for
262 confirmation and localization of the leak with the carpet method and subsequent underground
263 measurements.

264

265 **2.3.2 Attribution of leak indication signals from mobile measurements**

266 To attribute an observed leak indication (LI) from mobile measurements to a source category,
267 namely fossil, microbial and combustion, we used CO₂ and C₂H₆ signals, which were
268 continuously measured along with CH₄. We quantitatively evaluated C₂:C₁ ratios (%) when (i)
269 the CH₄ enhancements were larger than 0.5 ppm (ii) C₂H₆ enhancements were also larger than
270 15 ppb and (iii) the determination coefficient (R²) of the linear regression between CH₄ and
271 C₂H₆ was larger than 0.7. If CH₄ signals in mobile measurements were associated with CO₂
272 and high C₂H₆ mole fractions (C₂:C₁ > 10%), we attributed those emissions to combustion
273 (Maazallahi et al., 2020). When we repeatedly observed CH₄ enhancements, no CO₂
274 enhancements and C₂:C₁ ratios between 1 and 10%, or we observed persistent CH₄ signals in
275 several passes we did further on-foot inspection of the outlets. If the emissions from the outlets
276 clearly pointed to a fossil origin based on the CH₄ and C₂H₆ signals, we labeled the locations
277 as potential gas leak locations and reported them to the LDC for confirmation. We only
278 considered a location as a gas leak for further investigation if the LDC confirmed the existence
279 of a gas leak.

280 If at a particular location, we observed several CH₄ maxima, for example from different outlets,
281 we considered the “strongest” outlet as the main emission point. The “strongest” emission point
282 refers to a point where we observed the highest CH₄ mole fraction when the G4302 intake inlet
283 was put at a distance of ≈ 2 - 5 cm above the surface or outlet. When several emission outlets
284 with similar mole fractions were found, we considered the spatial average of the coordinates
285 as the main emission point. The tracer method then released C₂H₂ at the main outlet emission
286 point.

287 The LDC reported a C₂:C₁ ratio of 3.0% (96.20 ± 0.02 mol % CH₄ and 2.88 ± 0.00 mol %
288 C₂H₆, GNH personal communication) for the gas composition in the grid for the period of
289 August and September 2020 in Hamburg. This ratio was reported 3.5% (95.09 mol % CH₄ and
290 3.37 mol %, GNH personal communication) in April 2020.

291

292 **2.3.3 LDC leak detection and confirmation**

293 Since the pipeline locations are known to the LDC, the method can be applied precisely above
294 the pipelines, including visible cracks and cavity outlets in the close vicinity, increasing the
295 possibility of leak detection. Once the carpet method detects a CH₄ source, a second
296 measurement is performed above the location with the highest signal, where air is accumulated
297 and analyzed for the presence of C₂H₆. The C₂H₆ detection in the carpet method is not online
298 with higher detection threshold and in batch mode (gas chromatography), which takes time, 5
299 – 10 minutes per location. If sufficiently high CH₄ and C₂H₆ levels are found, the leak is
300 categorized in one of safety categories of A1, A2, B or C.

301

302 **2.3.4 Precise underground leak localization**

303 When a leak has been confirmed with the carpet method, a precise localization of the leak is
304 performed by drilling holes about 20-40 cm into the ground along the pipeline track and
305 measuring the sub-surface CH₄ concentration. The location with the maximum sub-surface
306 reading is assigned the most likely leak location where the repair teams open the road and
307 attempt repair of the leak. The final exact leak location is reported after opening ground for the
308 repair reactions. Mostly the locations reported from the carpet method matches the locations
309 reported from the leak repair team, which depends on the transport pathways of emission
310 undersurface and surface coverage.



311

312 **2.4 Emission quantification**

313 **2.4.1 Mobile measurements quantifications**

314 After the detection of the target locations, we performed additional transects at these locations
315 on different days. We accepted a mobile measurement transect of a leak location for further
316 analysis if (i) the GPS signals of transects were logged correctly along the street track and (ii)
317 at least one of the two instruments, G2301 (for quantification and attribution) and / or G4302
318 (for attribution), were running during the transect and (iii) the transect track included at least
319 one GPS coordinate less than 50 m from the leak location. The start and end point of the
320 accepted transects were determined as the locations where the driving tracks intersected with a
321 circle with radius of 100 m centered at the gas leak location reported by the LDC, or a reported
322 outlet location from the mobile method, for the locations where the LDC did not confirm a
323 leak. The segments between the start and end points were evaluated one by one (See an example
324 in Sect. S.4.1 in SI) to determine various parameters, e.g., the maximum CH₄ enhancements,
325 plume area, driving speed, distance to the actual leak locations, etc. The plume area is the
326 integral of the CH₄ enhancements above background along the driving track from the location
327 where the CH₄ enhancement exceeds > 10 ppb until the location where it falls again below the
328 10 ppb threshold.

329 Gas leak quantification from mobile measurements is based on an empirical equation derived
330 from controlled release experiments reported by von Fischer et al., (2017) and reevaluated in
331 Weller et al., (2019) (Eq. 1).

332

$$333 Q = \exp ((\overline{\ln (C_{max})} + 0.988) / 0.817)$$

Eq. 1

334

335 In Eq. 1, C_{max} is the maximum CH₄ enhancement (ppm) observed during each transect next to
336 the leak location. The maximum CH₄ enhancement should be more than 10% above CH₄
337 background level to be considered for the quantification algorithm. The emission rate is
338 denoted by Q and it is in L min⁻¹. $\overline{\ln (C_{max})}$ is the mean of the logarithm of the maximum
339 mole fraction enhancements for all accepted transects.

340 The standard quantification method only uses transects where CH₄ enhancements are more
341 than 10% or ≈ 200 ppb above background level. This 10% enhancement threshold corresponds
342 to about 0.5 L min⁻¹ emission rate in Eq. 1. Thus, ≈ 0.5 L min⁻¹ is the minimum emission rate
343 that can be quantified with Eq. 1 and leaks with smaller emission rates are ignored by design
344 of the method. Below we investigate the effect of relaxing the enhancement threshold. The
345 application of the tracer release technique in mobile mode allowed us to use the known C₂H₂
346 release rate and the measured C₂H₂ plumes to independently validate the mobile approach,
347 including the effect of the enhancement threshold. We also investigated the effect of distance
348 between CH₄ maxima to gas leak locations, which is not a parameter in Eq. 1.

349 The uncertainty of the emission rate for each location in the mobile method was calculated
350 using standard error and t-factor (95% confidence) for the locations with at least three CH₄
351 enhancements greater than the 10% threshold.

352 In addition to evaluating the maximum CH₄ enhancement from each transect we also derived
353 the plume area (mixing ratio times distance and in unit of ppm m) for comparison between the
354 instruments. In principle, the plume area should provide a more robust quantification of an
355 ambient CH₄ plume than the maximum enhancement: When a plume spreads out, individual
356 realizations of the plume can be sharper and higher, or wider and lower, depending on
357 meteorological conditions, but the plume area should be less affected. In addition, when an
358 instantaneous plume is sampled with two instruments with different gas flow rates, instruments
359 with a lower flow rate will be affected by mixing of air in the measurement cell. This will lead



360 to a lower maximum enhancement but a wider peak, and thus the peak area should lead to a
361 better comparison between the instruments.

362

363 **2.4.2 Tracer measurements quantifications**

364 The tracer method uses Eq. 2a to quantify CH₄ emissions in mobile mode (integral over space
365 dimension) and Eq. 2b in the static mode (integral over time dimension). Parameters relevant
366 for the evaluation with the tracer method are provided in Sect. S.4.2.

$$367 \quad Q_{CH_4} = Q_{C_2H_2} \cdot \frac{\int_{start}^{end} C_{CH_4} dx}{\int_{start}^{end} C_{C_2H_2} dx} \cdot \frac{MW_{CH_4}}{MW_{C_2H_2}} \quad \text{Eq. 2a}$$

$$368 \quad Q_{CH_4} = Q_{C_2H_2} \cdot \frac{\int_{start}^{end} C_{CH_4} dt}{\int_{start}^{end} C_{C_2H_2} dt} \cdot \frac{MW_{CH_4}}{MW_{C_2H_2}} \quad \text{Eq. 2b}$$

369

370 Here C is the mole fraction (ppm) and MW is the molecular weight of the species, 16 g mol⁻¹
371 for CH₄ and 26 g mol⁻¹ for C₂H₂. Q_{CH_4} is the CH₄ emission rate estimate for CH₄ (g s⁻¹) and
372 $Q_{C_2H_2}$ is the controlled release rate of C₂H₂ (g s⁻¹). The C₂H₂ flow rate was controlled and
373 measured with a flow controller (Brooks Sho-Rate). In addition, the mass of C₂H₂ released at
374 each location was measured by weighing the release cylinder before and after the tracer release
375 with a precise scale (KERN DE60K5A). The change in mass was then converted to a mass
376 flow rate using the release time. To convert the emission rate from mass (g s⁻¹) to volume (L
377 min⁻¹) we used normal temperature and pressure (NTP) conditions, T = 293.15 K, p = 1.01325
378 bar. The locations of tracer release (C₂H₂) at the confirmed gas locations were determined with
379 the combined information from the mobile and the carpet methods.

380 The tracer gas can also be used to pinpoint and confirm the emission source location. Prior to
381 quantification, it is important that the emission outlet is located for proper tracer release (see
382 Fig. 1) and source simulation and that other potential interfering emission sources can be ruled
383 out. This is secured by performance of upwind and downwind CH₄ mole fraction screening.
384 During transecting of the CH₄ and tracer plumes, the two plumes should match, if this is not
385 the case, the tracer release should be relocated until a proper plume match is obtained. If an
386 emission source consists of multiple outlets, the combined emission from all outlets can be
387 measured by releasing the tracer at the main outlet and increasing the measuring distance until
388 one confined overlapping plume of CH₄ and tracer gas is obtained. If the distance cannot be
389 increased to access limitations, tracer should be released at each single emission outlet.

390

391 **2.4.3 Suction measurements quantifications**

392 The quantification of a leak with suction method is possible after pumping accumulated air out
393 of soil and reaching CH₄ mole fraction equilibrium in the outflow. With the equilibrium CH₄
394 reached and the known pumping rate through the probes, it is then possible to calculate
395 emission rate (See Sect. S.4.3 in SI).

396

397 **2.4.4 Hole method, based on leak and pipeline properties**

398 The LDC reported the physical properties of gas leaks and pipeline conditions. These include
399 leak area, pipeline diameter and pipeline operational pressure. In order to get an estimate of the
400 upper physical limits of gas leakage through a hole with the given properties, we used the
401 empirical model by Liu et al., (2021), which was designed to quantify emissions from buried
402 natural gas pipelines to estimate emission rates from the leaks (Eq. 3), hereinafter “hole”
403 method.

404

$$405 \quad Q = 0.567 \cdot [(h + 139.592)^{-0.1} - 0.542] \cdot d^{1.5} \cdot p^{0.7} \quad \text{Eq. 3}$$

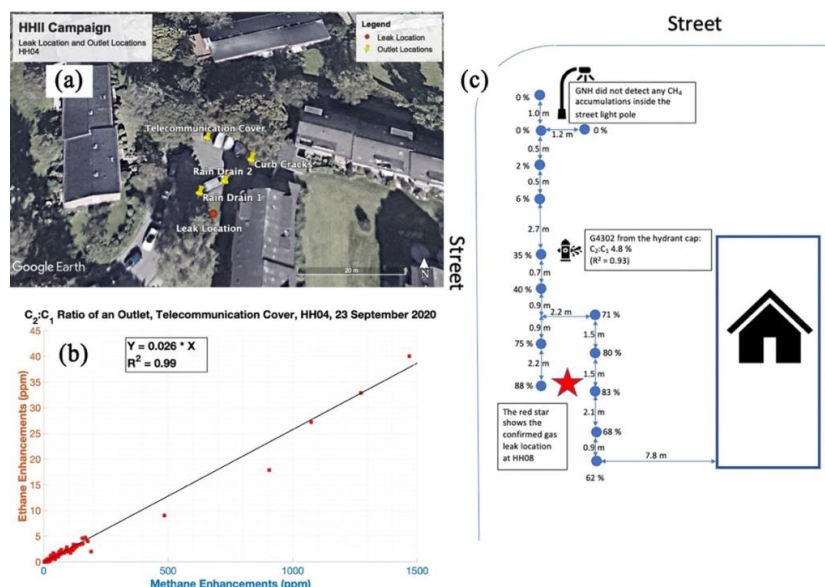


406
407 Here, Q is the gas leak rate in $\text{m}^3 \text{h}^{-1}$ (at standard atmospheric conditions and converted to
408 NTP), h is the depth of the buried pipeline in cm, d is the gas leak hole diameter in mm and p
409 is the pipeline overpressure in kPa. We used 150 cm as pipeline depth for all the locations in
410 Hamburg to estimate emission rate. We note that the model that we employed is for buried
411 pipelines not pipelines in open space, and emission estimates for the gas leak emission rate in
412 open space would be even higher (See Sect. 4.4 in SI). Ebrahimi-Moghadam et al. (2018)
413 showed that CH_4 emission from a pipeline hole area can be between 7 to 10 times higher in
414 open space relative to the subsurface conditions.
415

3 Results

3.1 Leak Detection

416
417
418 15 possible leak locations were detected by the mobile method in the initial surveys, (labeled
419 as HH001 – HH015). At 13 out of these 15 locations, leaks were confirmed by the LDC, HH007
420 and HH012 locations were not confirmed as gas leak locations. In addition, the LDC identified
421 5 other leak locations (labeled as HH100 – HH104) that had not yet been fixed (category B and
422 C). The overview of the measurements (detection and quantification) is provided in the SI (See
423 Sect. S.5 in SI). At some locations we also observed that vegetation was impacted negatively
424 by the presence of leaks in their vicinities, a known phenomenon as high levels of methane
425 cause harmful anoxic conditions for the plant roots (See Sect. S.6 in SI). At several locations
426 the outlet identification was straightforward, because we only observed one outlet, but at 5
427 locations we observed numerous outlets spread over a large area. Figure 2 shows the spread of
428 emission outlets at one of the locations (Fig. 2a), with correlations of CH_4 and C_2H_6 at the
429 “strongest” outlet (Fig 2b). Fig. 2c shows precise gas leak location practice of the LDC at one
430 of the other locations.
431



432
433 **Figure 2 – (a) aerial image of location HH004 (© Google Maps). Yellow pins show surface**
434 **emission outlet locations, and the red point shows the actual pipeline leak location**
435 **reported by the LDC; (b) correlation between CH_4 and C_2H_6 measured from a**



436 telecommunication cover; (c) Map (not to scale) of drilled holes (blue dots) to locate the
 437 pipeline gas leak at HH008. The red star shows the actual pipeline gas leak location as
 438 indicated by the undersurface CH₄ mole fractions (See Sect. S.3, Fig. S3)
 439

440 3.2 Leak Quantification

441 Table 1 shows the results of the leak emission rate quantifications from the four methods. All
 442 these locations were quantified by the mobile method, although for 6 of them the 10%
 443 enhancement threshold was not reached. 16 locations were quantified by the tracer release
 444 method and 8 by the suction method. A complete overview of key parameters for all
 445 measurements (detection and quantification) is provided in Sect. S.5.
 446

447 Table 1 – Results of gas leak quantification with different methods in Hamburg, Germany

	ID	Leak quantification methods (L min ⁻¹)							Info. from the LDC			
		Mobile (measurements from G2301)			Tracer (L min ⁻¹)	Suction		Hole (L min ⁻¹)	Pipeline buried year	Leak size (cm ²)	Leak type; Safety considerations	Pipeline Size and Material#
		Transect (s) w/ CH ₄ Enh. > 10% threshold	Emission average	Emission range; 95% confidence		Emission (L min ⁻¹)	Status					
Detected by mobile method	HH001	n = 1 (10%)	0.7	-	0.06	<1.8	INC	39	1935	2.5	C	DN80ST
	HH002	n = 5 (50%)	4.9	0.7 – 36.0	0.22	<0.7	INC	45	1935	3.0	A2	DN80ST
	HH003	n = 6 (86%)	7.5	1.1 – 53.0	1.37	-	-	-	1963	-	A1	DN100ST
	HH004	n = 4 (100%)	7.8	1.8 – 34.5	5.33	-	-	-	1959	-	A1	DN80ST
	HH005 ⁺	n = 19 (51%)	1.8	0.9 – 3.6	0.21	-	-	-	1935	-	A2	DN80ST
	HH006 [*]	n = 11 (39%)	1.2	0.8 – 1.8	0.02	0.3	CPLT	33	1934	0.5	B	DN80ST
	HH007 [°]	n = 0 (0%)	-	-	-	-	-	-	-	-	-	-
	HH008	n = 6 (26%)	1.5	0.4 – 6.4	0.32	<1.3	INC	-	1934	-	C	DN80ST
	HH009 [×]	n = 9 (38%)	3.9	1.5 – 9.8	4.86	<3	INC	-	1928	-	A1	DN80ST
	HH010	n = 3 (38%)	1.6	0.2 – 13.7	0.51	<0.7	INC	-	1937	-	C	DN200ST
	HH011 [^] ×	n = 4 (50%)	1.9	0.2 – 18.6	0.37	-	-	150	1963	15	A1	DN300ST
	HH012 [°]	n = 0 (0%)	-	-	-	-	-	-	-	-	-	-
	HH013 [^]	n = 2 (40%)	1.8	-	-	-	-	65	1939	5	A1	DN80ST
	HH014	n = 24 (55%)	1.6	1.1 – 2.5	1.41	-	-	65	1950	5	A1	DN100ST
	HH015	n = 1 (50%)	1.0	-	0.38	<0.9	INC	19	1935	1	A1	DN80ST
Reported by the LDC	HH100	n = 1 (13%)	0.7	-	0.14	-	-	-	1994	-	C	d225Pe
	HH101	n = 0 (0%)	-	-	0.07	<0.7	INC	-	1960	-	C	DN80ST
	HH102	n = 0 (0%)	-	-	0.01	-	-	-	1928	-	C	DN125ST
	HH103	n = 0 (0%)	-	-	0.03	-	-	-	1963	-	B	DN150ST
	HH104	n = 0 (0%)	-	-	-	-	-	-	1930	-	C	DN100ST

448 ⁺ The LDC reported three leak locations, ≈ 30 m distance between the two ends, for this
 449 location: two leaks with area of 5 cm² and one leak with area of 1 cm²

450 ^{*} Complete measurements for the suction method and used for averaging

451 [^] Leak size reported as sum of total hole area of all the leaks on the pipeline

452 [×] Large difference between leak location and the tracer release location

453 [°] The LDC did not confirm a gas leak

454 [#] Pipeline materials, steel (ST) or Polyethylene (Pe), pipeline Diameter Nominal (DN),
 455 which is close to the inner pipeline diameter in mm



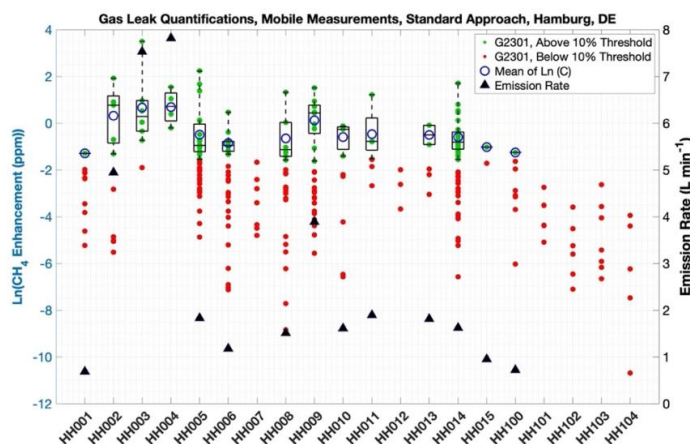
456

457 3.2.1 Mobile method

458 The mobile method was applied at all the 20 locations (18 confirmed and 2 unconfirmed gas
459 leak locations). At 14 (all confirmed gas leak locations) out of the 20 locations, CH₄
460 enhancements above the 10% threshold were observed and could be evaluated with the
461 standard algorithm. The emission rate estimates for these 14 gas leak locations ranged from 0.7
462 to 7.8 L min⁻¹. At the 6 other locations we didn't observe any CH₄ enhancements above the
463 10% threshold. When we lowered the enhancement threshold to 10 ppb, the emission rates
464 were 0.07 (HH007; not confirmed gas leak location), 0.1 (HH012; not confirmed gas leak
465 location), 0.04 (HH101), 0.02 (HH102), 0.05 (HH103) and 0.02 L min⁻¹ (HH104). Of the 5
466 leak locations reported by the LDC, 4 did not show any enhancement maximum above the 10%
467 threshold, i.e., these locations would not have been identified with the default algorithm
468 (Weller et al., 2018) and would thus not produce an emission estimate.

469 Fig. 2 shows a summary of all individual observed enhancement maxima with the G2301
470 analyzer from all transects with the mobile vehicle, which were used for the quantification of
471 emission rates with Eq. 1. The figure illustrates the large spread in enhancement maxima for
472 multiple passes at each location, similar to Luetschwager et al (2019), leading to large
473 uncertainties in emission estimates of individual locations. Fig. 2 also shows the diversity of
474 the various locations, where at some locations most or all of the observed enhancement maxima
475 are above the 10% threshold (e.g. HH003 and HH004), at several locations none of the
476 enhancement maxima was above the threshold (e.g. HH101 and HH104) and at other locations
477 many transects showed enhancement maxima both above and below the threshold (e.g. HH006,
478 HH008, HH009, HH014).

479 As shown in Fig. 3, there is a wide range of CH₄ enhancement observations per location. This
480 depends on wind conditions, distance of the observed plume maximum to the emission outlet
481 location, the superposition of emissions from several outlets and likely other variables such as
482 soil water content. The mean relative uncertainty from the mean emission rate values for the
483 mobile method is $\approx 70\%$ for lower and 400% for the upper ends for the locations with at least
484 3 transects (n = 10) which pass the 10% enhancement threshold (significant signals) in this
485 study. The lower and upper ranges go down to 60% and 275% for the locations with at least 5
486 transects (n = 7) with significant CH₄ enhancements.



487

488

489

490

Figure 3 – CH₄ enhancement maxima from all individual transects for each location using G2301. Red points show CH₄ enhancement maxima below the 10% threshold, green points show CH₄ enhancement maxima above the 10% threshold, thus used for the



491 **standard quantification. Blue circles show the $\overline{\text{Ln}(C_{max})}$ of all the green points for each**
492 **location, and black triangles show the derived mean emission rate (based on all green**
493 **points) using Eq. 1 for the location with at least one green point (right y-axis).**

495 3.2.2 Tracer method

496 The tracer method performed emission rate quantification at 16 gas locations out of 20
497 locations. The derived emission rates range from 0.03 to 5.3 L min⁻¹ (Table 1). For 4 locations
498 the tracer method was not applied because (i) the emissions were not persistently observable
499 and the LDC also didn't confirm existence of gas leaks at these locations (n = 2; HH007 and
500 HH012) or (ii) the leak had already been repaired (n = 1; HH013) or (iii) no emission was
501 detectable during the visit of the tracer team (n = 1; HH104). For two of the locations (HH11
502 and HH09), where leaks were confirmed and the tracer method was successfully deployed,
503 later investigations during repair actions (see Fig. 1) showed that the surface emission outlets
504 were located far (15 to 60 m) from the actual gas pipeline leak location indicating underground
505 gas migration. It is evident from Table 2 that the tracer technique can also quantify very small
506 emission rates, below the cut-off of the mobile technique of 0.5 L min⁻¹. Emission rate
507 estimates derived from the tracer technique were in general lower than the ones derived from
508 the mobile technique, except for three sites where they were comparable (HH004, HH009 and
509 H014).

511 3.2.3 Suction method

512 Due to the time-consuming nature of the suction measurements, initially 10 gas leak locations
513 had been planned for deployment of the suction method in this campaign. The goal was to
514 cover a wide range of expected emission rates, as stated in the intercomparison matrix. The
515 suction method was applied at 8 gas leak locations (see Table 1) out of which the suction
516 quantification was complete (HH006) according to protocol where an equilibrium
517 concentration has to be reached. This was at HH006, with a derived emission rate of 0.3 L min⁻¹.
518 At several of the locations where the mobile method had indicated high emission rates,
519 subsurface accumulation was widespread, and the suction method was either not deployed (n
520 = 3; HH003, HH04, HH011) or the measurements were incomplete (n = 7; HH001, HH002,
521 HH008, HH009, HH010, HH015 and HH101) because of either safety reasons or because the
522 suction team estimated that they would be unable to complete the measurements within a day.
523 For the 7 locations with incomplete suction measurements, the emission rates were reported
524 ranging from 0.7 to 3 L min⁻¹. These can be regarded as upper limit estimates because suction
525 was not yet completed and CH₄ concentrations would have supposedly dropped further.

527 3.2.4 Hole method

528 For 5 locations where the leak area of a single gas pipeline leak was reported, the corresponding
529 emission rates are between 19 to 65 L min⁻¹. For locations HH011 and HH013, the hole area
530 was reported as the sum of several holes and the total hole area for these two locations resulted
531 in an emission rate of 150 and 65 L min⁻¹, respectively. The quantification from the hole method
532 is higher than from the mobile, tracer and suction methods by at least an order of magnitude.

534 3.3 Leak categories

535 The 20 (18 confirmed + 2 not confirmed) locations can be divided into four main categories
536 related to measurement challenges of the various methods. These categories may overlap.

- 537 (i) Large subsurface CH₄ accumulation
- 538 (ii) Insufficient CH₄ enhancements for mobile quantification
- 539 (iii) Large CH₄ enhancement variability for mobile quantification
- 540 (iv) Several outlets and / or leaks or atmospheric turbulence



541 In this section we present the overall results and discuss in detail one selected location for each
542 of these categories. The remaining locations (with similar characteristics) are presented in the
543 SI.

544

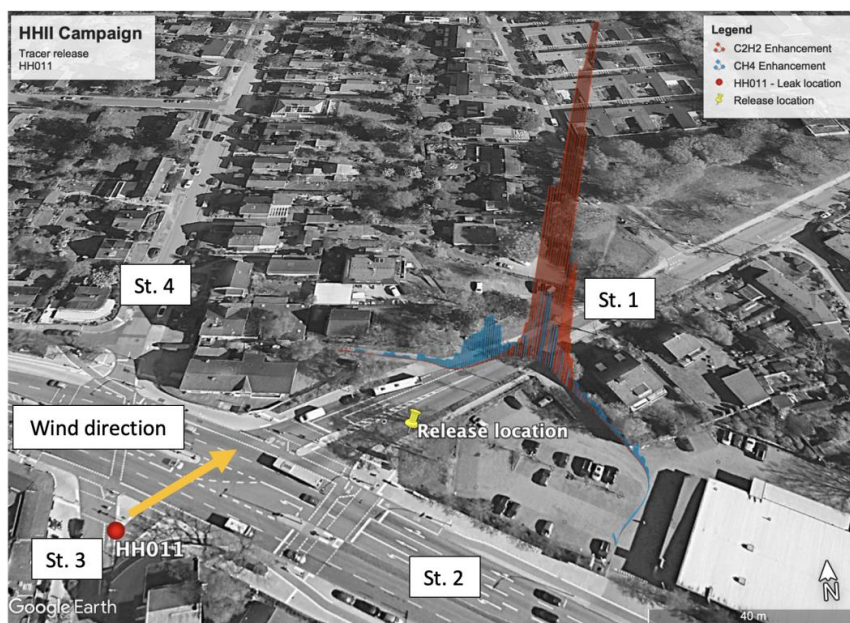
545 **3.3.1 Location type I – Large subsurface CH₄ accumulation and multiple outlets**

546 The spatial spread of surface emission outlet locations identified with the G4302 instrument as
547 part of the mobile method provides an indicator for the extent of the subsurface accumulation
548 of CH₄. For 5 locations, emission outlets were found at great distance from each other, in order
549 of tens of meters. The total emission of a gas leak is equal to the sum of emissions from all the
550 surface outlets at a location, thus it is necessary to quantify each outlet separately to get the
551 total emission.

552 HH011 (Fig. 4) is an example where very widespread CH₄ accumulation and migration was
553 observed. During the initial mobile gas leak detection, leaks were located at the intersection of
554 streets 1 and 2, close to a subsurface vent and a rain drain, ≈ 2 m far apart, (the yellow pin in
555 Fig. 4a) based on clear signals from these outlets and a sign next to the road indicating presence
556 of gas pipelines. The vent showed a C₂:C₁ ratio of 2% (R² of 0.8 and max CH₄ mole fraction
557 of 31 ppm) and we observed C₂:C₁ ratio of 2.8% with R² of 0.96 and max CH₄ mole fraction
558 of ≈ 70 ppm from the rain drain, clearly indicating a large / dominant contribution from fossil
559 CH₄. However, after quantifying the emission from these two leaks using the mobile and the
560 tracer release methods, the LDC found the actual gas pipeline leak, during the repair actions,
561 on the south side of the intersection, far from the vent and the rain drain, at the intersection of
562 street no. 3 and no. 2 indicating that the gas had travelled about 60 m underground. It is possible
563 that the leak resulted in several gas emission outlets, likely closer to the gas pipeline leak
564 location. The emission rate measured using the mobile method was 1.6 L min⁻¹ based on 5
565 plume transects and is likely underestimated because some emission outlets potentially were
566 not included in the performed plume transect. It should also be noted that the distance from the
567 gas pipeline leak location to the plume transect is larger than the distances applied during the
568 controlled release calibrations (average 15 m) (Weller et al., 2019).

569 The tracer was released at the vent and the rain drain and thus measured the combined emission
570 from these two outlets to be 0.4 L min⁻¹. If the gas pipeline leak gave rise to multiple
571 unidentified surface emission outlets, the emission from the gas pipeline is underestimated. IN
572 fact, Fig. 4b shows that a CH₄ plume without C₂H₂ was observed during the tracer release
573 measurements at HH011, confirming that at least one other source of methane emission was
574 present nearby.

575 Based on the previous experience at locations with widespread subsurface accumulation it was
576 concluded that the suction method could not be applied at this location. The other case in this
577 category was HH009.



578
579 **Figure 4 – aerial image of HH011 (© Google Maps). A gas leak location with widespread**
580 **undersurface CH₄ accumulation. The yellow pin shows the assumed leak location and**
581 **location of tracer release, which was very different from the actual leak location as**
582 **identified by the LDC (red circle). St. 1-4 are added to identify streets that are discussed**
583 **in the text. General wind direction during tracer release deployment is shown with an**
584 **orange arrow. CH₄ (in blue) and C₂H₂ (in red) levels measured at a plume transect. One**
585 **of the CH₄ plume is proportional to the C₂H₂ plume while the other CH₄ plume lacks the**
586 **C₂H₂ signals suggesting existence of at least another emission outlet.**

587
588 The LDC reported the total area of several holes in the pipeline as 15 cm² for HH011, which is
589 the largest leak size among all the locations. If we assume that there was one hole with this
590 size, then the emission rate estimated by Eq. 3 will be 150 L min⁻¹, a hole of 5 cm² gives
591 emission rate of 65 L min⁻¹. The pipeline for this location was DN300ST and has been in
592 operation since 1963.

593 594 **3.3.2 Location type II – Insufficient CH₄ enhancements for mobile quantification**

595 At HH101, on a narrow (≈ 3 m wide) street, which had about 1 m wide bare soil pavement on
596 one side, the LDC reported a gas leak location based on their routine surveys. On both sides of
597 the street there were about ≈ 1.5 m tall bushes and some trees. All three methods (mobile, tracer
598 and suction method) were deployed at this location. Gas emissions found their way to the
599 atmosphere through cracks in the asphalt with C₂:C₁ ratio of 2.5% (R² of 0.93) with max CH₄
600 mole fraction of ≈ 25 ppm. None of the CH₄ enhancement maxima observed during the mobile
601 surveys at this location were above the 10% enhancement threshold with the G2301 instrument,
602 thus this location would not be labeled as LI and no quantification would be reported from
603 mobile method as implemented in Weller et al (2019) and Maazallahi et al. (2020). The tracer
604 method was applied in static mode at a distance of ≈ 15 m and reported an emission rate of 0.1
605 L min⁻¹, which is compatible with the emission strength being below the “detection limit”
606 defined by the 10% cut-off of the standard algorithm (0.5 L min⁻¹). When the emission strength
607 is evaluated using the CH₄ enhancements below the cut-off, the value is 0.04 L min⁻¹. The



608 suction method was applied at this location but an equilibrium was not achieved after 9 hr, i.e.
609 incomplete suction measurements, and an upper limit for the emission rate of $\approx 0.7 \text{ L min}^{-1}$ was
610 reported. The fact that the suction measurement was incomplete at this location with a small
611 emission rate shows that subsurface accumulation can also be large for smaller leaks.

612 Three of the leak locations in this study only showed one CH_4 enhancement above threshold.
613 The 10% threshold is a constraint, which removes enhancements less than about 200 ppb. This
614 means for the locations where we only have one transect with CH_4 enhancements more than
615 the 10% threshold, the minimum emission rate estimated is about 0.5 L min^{-1} , no matter how
616 many transects we had with CH_4 enhancements less than the 10% threshold. This situation was
617 observed for HH001, HH015 and HH100 (Fig. 5). In this case, the mobile method likely
618 overestimates the total leak rate, because only the maximum enhancement is used for
619 quantification. The tracer method reported low emission rates for these three sites 0.12 L min^{-1}
620 on average ($n = 6$).

621 For the two locations (HH007 and HH012) where the LDC didn't confirm gas leaks (despite
622 periodic observation of C_2H_6 at outlets during the mobile surveys) none of the transects showed
623 CH_4 enhancement maxima above the 10% threshold. At HH007, the outlet was through cracks
624 in the pavement but at HH012 the outlets were from manholes. At HH007 the outlet location
625 had shifted by about 2 m for two different days (4-week gap). We note that the correlation
626 coefficients between CH_4 and C_2H_6 at these locations were between 0.4 and 0.6, so less than
627 0.7, which is the threshold correlation we accepted for the outlets. As a leak was not confirmed
628 for these locations, the tracer and suction methods were not applied.

629

630 3.3.3 Location type III – Large CH_4 enhancement variability for mobile quantification

631 For several locations, we observed a large variability of CH_4 enhancements from different
632 transects. One example is HH008, where only 6 of the 23 transects exceeded the 10% threshold,
633 i.e. the leak was only observed in about every 4th transect. The leak location of HH008 is an
634 example where CH_4 enhancements from several transects cover a wide range. Based on the 6
635 transects, which showed enhancement maxima above the 10% threshold, a leak rate of 1.5 L min^{-1}
636 is derived. This may be an overestimate since many transects with maxima below the
637 threshold were not considered. For this location the mobile tracer method was applied, which
638 resulted in a leak rate quantification of 0.3 L min^{-1} .

639 The suction method derived an upper emission estimate of 1.3 L min^{-1} from incomplete
640 measurements at HH008. The LDC reported a C category leak for this location from a DN80ST
641 pipeline, which was installed in 1934.

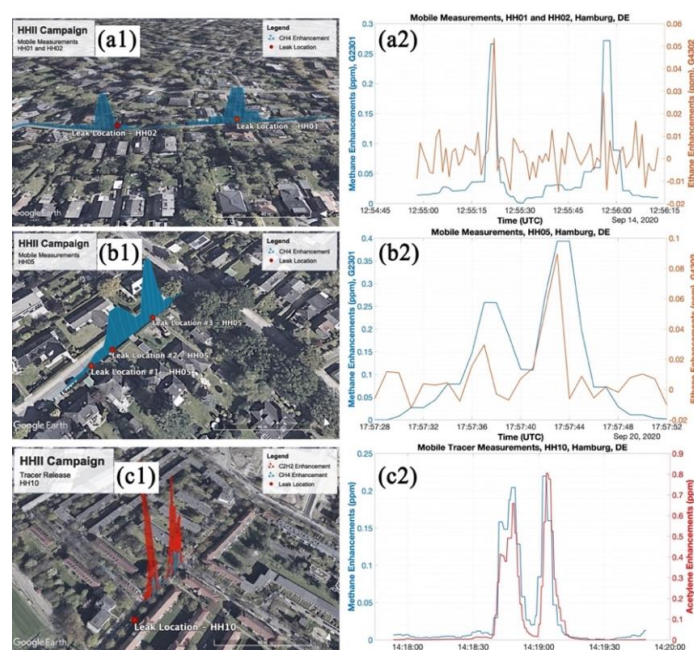
642

643 3.3.4 Location type IV – Several outlets and / or leaks or atmospheric turbulence

644 On a $\approx 5 \text{ m}$ wide street, we detected two leaks about 80 m away from each other, HH001 and
645 HH002 (Fig. 5a). It was a cobblestone street and there were bushes and few trees planted,
646 mostly on one side of the street. The mobile method performed 10 transects at both locations
647 and all the transects were accepted for the evaluation. The tracer team could quantify both
648 locations using static measurements. The suction team began to quantify HH002 and HH001,
649 but during quantification of HH001, there was a small accident (fire due to contact of drilling
650 head with electric cable) and the leak had to be fixed immediately. The plumes on this street
651 were sufficiently separated to positively identify two different leaks on the same street. In
652 contrast, at location HH005, we observed several maxima for the same transect, but because
653 the maxima were close to each other, those were clustered together in the mobile measurement
654 algorithm (Fig. 5b). Later the LDC reported even three individual pipeline leaks on this street.
655 In another example (HH010), some transects showed several plume maxima although only one
656 emission outlet and later on only one gas pipeline leak was found (Fig. 5c). However, the
657 release of the tracer resulted in several matching CH_4 and tracer gas plumes confirming that



658 the emission indeed occurred from a single outlet and that the multiple plumes at this location
659 were due to inhomogeneous plume dispersion. This illustrates that the existence of several
660 maxima in one transect does not necessary correspond to presence of several leaks and/or
661 outlets, but it can also be related to a spatially heterogeneous/disturbed plume. This shows that
662 the signals from the mobile detection method are not sufficient to allow determining the
663 number of leaks at a location with several plume at a close distance from each other in a single
664 transect.
665



666 **Figure 5 - several maxima observed during a single transect on one street showing**
667 **different situations: two well isolated leaks with about 80 m distance from each other (a1**
668 **and a2, HH001 and HH002), three pipeline leaks close to each other with several emission**
669 **outlets (b1 and b2, HH005) and one leak and one outlet but several CH₄ enhancement**
670 **maxima due to turbulence (c1 and c2, HH010), aerial images: © Google Maps.**
671
672

673 After detection by mobile measurements, emissions out of the ground were detected at HH001
674 and HH002 with the G4302 backpack within 3 m distance from the gas pipeline leak locations,
675 which was later reported by the LDC. For the single transect with a maximum above the 10%
676 threshold observed with the mobile method, the derived emission rate at HH001 was 0.8 L min^{-1}
677 ($n = 1$). For HH002, the derived emission estimate for the transects with maxima above the
678 threshold is 5.2 L min^{-1} ($n = 5$) from the mobile method. At HH002, individual derivation of
679 emission from separate CH₄ enhancement gives a wide range between 0.7 and 36.0 L min^{-1}
680 (95% confidence) from the mobile method (see category III above). For HH001, the tracer
681 method was applied in static mode at $\approx 30 \text{ m}$ distance to the release point and $\approx 40 \text{ m}$ far from
682 HH002. The derived emission rate for HH001 is 0.06 L min^{-1} and for HH002 0.22 L min^{-1} from
683 the tracer method. For HH001, after about 5 hr of pumping, the suction quantification had to
684 be stopped due to the incident described above. Based on the incomplete suction measurement
685 an upper limit for emission rate of $\approx 1.8 \text{ L min}^{-1}$ for HH01 was estimated. An emission estimate
686 of $\approx 0.7 \text{ L min}^{-1}$ was derived for HH002 from an incomplete suction measurement. The LDC

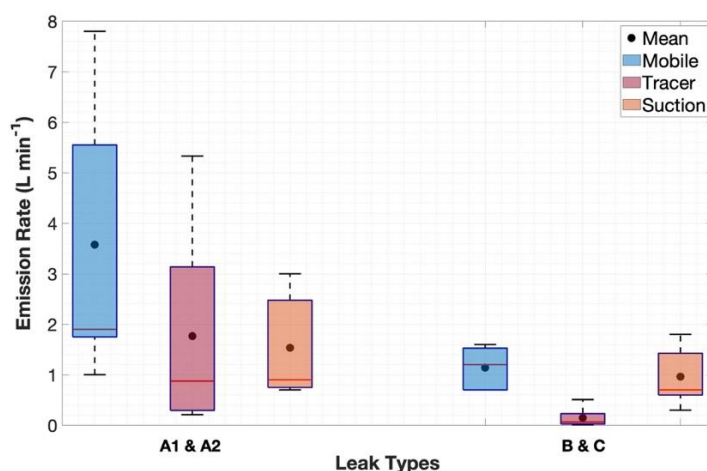


687 reported leak size of $\approx 2.5 \text{ cm}^2$ for HH001 and for $\approx 3 \text{ cm}^2$ for HH002 which then give emission
688 rate of 39 and 45 L min^{-1} respectively from the hole method. For both locations, leaks were due
689 to pipeline corrosion.

690

691 3.4 Emission rates of different leak safety types

692 The 18 confirmed gas leak locations that were investigated in the campaign were categorized
693 into the four safety categories, A1 ($n = 7$), A2 ($n = 2$), B ($n = 2$) and C ($n = 7$). The mobile
694 method quantified all the A1 and A2 leaks ($n = 9$) with an average emission rate of 3.6 L min^{-1} .
695 5 out of 9 leaks in categories of B and C leaks were quantified with the mobile technique
696 including the 10% threshold with average emission rate of 1.1 L min^{-1} ($n = 5$). Apart from one
697 location, which had to be fixed before the measurements, the tracer method quantified the A1
698 and A2 leaks ($n = 8$) and reported an average emission rate of 1.8 L min^{-1} . The tracer method
699 also quantified all the B and C leaks ($n = 9$) with an average emission rate of 0.1 L min^{-1} .
700 Mostly due to the safety and time constraints and medium to large underground accumulations
701 of CH_4 , the suction method could provide incomplete measurements at only 3 locations of A1
702 and A2 leaks with an average emission rate of 1.5 L min^{-1} ($n = 3$). The suction method measured
703 at 5 out of 9 B and C locations, one of the measurements was complete and the others were
704 incomplete, with an average emission rate of 1.0 L min^{-1} ($n = 5$). Although the number of
705 quantified leaks is limited, all the three methods show that the emission rates from category A1
706 and A2 leaks are higher than category B and C leaks (Fig. 6). This indicates that the site
707 selection bias of measurements for the suction method due to safety concerns (see qualifier
708 above), can lead to a bias in the emission rate in this method.



709

710 Figure 6 – Emission rate differences between different gas leak categories

711 4 Discussion

712 4.1 Leak detection methods

713 4.1.1 Leak location vs outlet location

714 There is a difference between the location of the leak in the gas pipeline (leak location; See
715 Sect. S.7 in SI) and the location where the gas is emitted to the atmosphere (outlet locations;
716 See Sect. S.2 in SI). Furthermore, a single leak in the gas pipeline can result in multiple
717 emission outlets at the surface. In this campaign we observed that in most cases (2 out of 18),
718 the emission outlet at the surface occurred only a few m (sometimes $< 1 \text{ m}$) from the location
719 of the leak in the gas pipeline. However, in one case, an emission outlet was detected about 60



720 m away from the leak location indicating significant underground gas accumulation and
721 migration (see Fig. 4).

722

723 **4.1.2 Intercomparison of the gas leak detection methods**

724 The mobile method detects atmospheric CH₄ enhancements while measuring continuously with
725 ppb precision from an inlet installed at the front bumper of the car while LDCs apply the carpet
726 method with an instrument precision at the ppm level. High precision for the carpet method is
727 not needed as the inlet to their instruments is connected to a carpet, which is attached to the
728 ground. The mobile method can cover larger areas in shorter times, but not all roads, walkways,
729 or other surface areas where pipelines are buried are accessible with a vehicle. The advantage
730 of the carpet method is that it can precisely follow the pipeline map, which also means that it
731 can locate leaks more precisely. The mobile method use a 10% threshold to neglect unreliable
732 gas leak sources, which sometimes results in neglecting actual signals from small leaks. Also
733 the mobile measurements do not detect all leaks due to the dependence on the wind direction
734 (only downwind sources leaks can be detected). Luetschwager et al. (2021) suggested that 5 to
735 8 plume transects give > 90% probability of gas leak detection at a given location, so if all the
736 streets in an urban area are covered 5 to 8 times, > 90% of the leaks can be detected by mobile
737 measurements.

738 Both the mobile and the carpet method use C₂H₆ signals for distinguishing between fossil and
739 microbial CH₄ emissions, and as for C₂H₆, the instrument used in the mobile method is more
740 sensitive, and faster. In the carpet method, the laboratory analysis of C₂H₆ is slow and with
741 higher detection threshold compared to the mobile method, where C₂H₆ is measured in real-
742 time during the surveys, and also on foot from the emission outlet. The CRDS instrument
743 provides real-time measurements of CH₄ and C₂H₆ at 1 Hz frequency so checking various
744 outlets at a possible gas leak location is faster.

745 At 14 out of the 20 locations in this study, gas leaks were detected (CH₄ signals passing the
746 10% threshold) and quantified with the mobile method. However, we observed that 4 out of 5
747 locations reported by the LDC would not have been detected in mobile surveys without prior
748 information on existence of the leaks because the maximum enhancement was below the
749 mobile detection threshold. At the only location (HH100) from the list of the LDC, where
750 mobile method could quantify the emissions, the outlets were located on the road and the
751 vehicle was driving on top of the outlet. For this location only one of the transects passed the
752 10% enhancement threshold, and the quantification for this location was $\approx 0.7 \text{ L min}^{-1}$, close
753 to the detection threshold of this method, $\approx 0.5 \text{ L min}^{-1}$. One of the other locations, HH101,
754 reported by the LDC had similar surrounding conditions (e.g. presence of buildings, road
755 conditions, etc.) as the other leaks detected by the mobile method, but still the mobile method
756 was not able to detect a gas leak at this location without a priori information from the utility.
757 The quantifications made by the tracer method suggest that the emission rates of the locations
758 provided by the LDC were much lower than the locations detected by mobile measurements
759 (Table 2). The 10% threshold in the mobile method precludes the identification of small leaks
760 ($< 0.5 \text{ L min}^{-1}$), which would only be identified by the carpet method.

761

762 **4.2 Signal attribution in mobile detection method**

763 **4.2.1 Attribution during mobile survey in car**

764 During the mobile measurements we used two approaches to find correlation between CH₄ and
765 C₂H₆. When we compare the online measurements point by point, the probability of detecting
766 a fossil signal is high, as only one single significant reading is sufficient to indicate a fossil
767 signal. When we use the R² of the linear correlation between CH₄ and C₂H₆ enhancements
768 above the cut-off, the attribution is more reliable. In a large dataset without a priori information



769 on the existence of a gas leak at different locations, the correlation method is more trustworthy
770 as the point-by-point method could be affected by instrument noise and/or spikes.
771 We also used CO₂ signals and their correlation with CH₄ signals to investigate interference
772 from combustion or microbial processes. For only 7 plumes at 6 locations, we detected
773 correlations between CO₂ and CH₄, which could indicate either oxidation of CH₄ to CO₂ or
774 mixture of microbial CH₄ emissions from e.g. the sewer system with the emissions from natural
775 gas leaks. The number of these possible co-emissions is low compared to the number of total
776 transects (only $\approx 7\%$ of the plumes with CH₄ enhancements greater than 10%), thus such an
777 admixture of microbial CH₄ should not impact the quantification from mobile method
778 significantly.

779

780 4.2.2 Plume attribution to emission outlets

781 The outlet attribution was performed using the G4302 CRDS instrument which is portable like
782 a backpack. We checked the outlets (See Sect. S.2, Fig. S1) around the locations of interest and
783 evaluated the correlation between CH₄ and C₂H₆ and the persistence of the emissions on
784 different days. In theory, it is possible to estimate contributions of fossil and microbial CH₄ in
785 a plume using the ethane signals during the mobile measurements with the vehicle and the
786 reference C₂:C₁ ratio provided by the LDC. However, due to the low C₂H₆ signals in ambient
787 air, it was not feasible to quantify the possible contribution of microbial methane emissions.
788 Nevertheless, the C₂H₆ signals of the G4302 CRDS instrument were still very useful to identify
789 a location as a possible gas leak location or not. For all the 15 locations, which were initially
790 detected by the mobile method we observed detectable C₂H₆ signals, including the two
791 locations which later were not confirmed as a gas leak location by the LDC. This suggests that
792 either the leak is at a greater distance and depending on the transport of the emission we
793 periodically can see the signals at the detected outlets or that there are sources that produce
794 both CH₄ and C₂H₆ in the vicinity of the location.

795

796 4.3 Leak quantification methods

797 4.3.1 Mobile method

798 If the outlets are close to each other, we may observe several CH₄ enhancements close to each
799 other or overlapping when a single transect is performed at a close distance. If we assume that
800 the number of CH₄ maxima is equivalent to the number of real outlets that exist on a road and
801 only use the maximum enhancements from the most pronounced plume to calculate the
802 emission rate, the total emission will be underestimated with the mobile method.

803 Emission rate estimates with the mobile method from individual transects are associated with
804 high uncertainty, related to variabilities in either above-ground or under-ground conditions. For
805 example, an unfavorable wind direction (above ground condition) can result in missing a plume
806 from a gas leak. The mobile measurement van itself may also affect the measurement, e.g., by
807 creating pressure fluctuations. Luetschwager et al. (2021) showed that the quantifications from
808 the same leak in individual mobile transects can vary by more than an order of magnitude. In
809 Hamburg, we found that the range can be even a factor 50 or 100 in exceptional cases (Table
810 2). This high variability illustrates that if we perform only one transect per location, the
811 estimated leak emission rate can result in high under / overestimation in emission estimate for
812 the single location, as was also reported by Maazallahi et al. (2020). This large uncertainty for
813 individual locations is less severe when the results are extrapolated to the city-level, where the
814 sample size is also large, including over- and underestimates (Brandt et al., 2016).

815 In our previous study in Hamburg (Maazallahi et al., 2020) the overall average emission rate
816 for all the LIs was estimated 3.4 L min⁻¹ LI⁻¹ (n = 145) while for the fossil-attributed
817 locations it was 5.2 L min⁻¹ LI⁻¹ (n = 45; standard error of 3.1). This showed that the biggest
818 emitters were among the fossil categories. In the present study, the average emission rate from



819 mobile measurements for the gas leak locations is $2.7 \text{ L min}^{-1} \text{ LI}^{-1}$ ($n = 14$; standard error of
820 0.6). The higher average emission rate per fossil location in the first campaign may have been
821 caused by the fact that in that campaign only a smaller number of transects were performed per
822 location (on average 1.1 in the previous study versus 6.9 transects with $\text{CH}_4 > 10\%$ threshold
823 per location in the present study). Luetschwager et al. (2021) stated that after 6 transects with
824 CH_4 exceeding the 10% threshold per location the average overestimation of leak size estimates
825 will be less than 10%. In addition, the differences in sample size and locations in these two
826 studies (45 versus 14 locations in the first and second studies respectively) may partially
827 explain the difference in average. This is because the probability of detecting large emitters,
828 which increase the average emission rate of all leaks, increases with sample size.

829 The two CH_4 sensors onboard the mobile van play specific roles in the detection and
830 quantification of leaks. CH_4 enhancements on the G2301 are 3.8 times lower than the G4302.
831 This is an artefact of the G2301, which smoothes the signal compared to the G4302 because of
832 the slower pump and sampling rate (See Sect. S.8.1 in SI). On the other hand, this results in
833 more signals passing the 10% threshold on G4302. This then also leads to higher detection
834 probabilities using G4302 (See Sect. S.8.2 in SI). Higher record of CH_4 enhancements then
835 also results in higher emission rate quantification using Eq. 1 (See Sect. S.8.3 in SI). We use
836 the G2301 for quantification, since this is the instrument that was also used for introduction of
837 the mobile equation quantification in Weller et al. (2017). The quantification of the gas leak
838 locations using Eq. 1 depends only on the CH_4 enhancements. This gives about a factor 2 higher
839 emission rates from G4302 than from G2301 for the same plumes. When we evaluate the plume
840 areas from the two instruments, they are much closer to the 1:1 line (See Sect. S.8.3 in SI). This
841 agrees with findings from another study using two different in-situ instruments onboard a
842 mobile car (See Sect. S1.5, Fig. S6 from Ars et al. (2020)). They also found that the plume area
843 is closer to the 1:1 line in mobile measurements even if the air intakes are not at the same
844 location of the vehicle. This suggests that the plume area is a more robust parameter than
845 maximum enhancement for emission rate quantification and a leak rate quantification equation
846 using the plume area should be developed.

847 In general, the closer the air intake is to the emission point the higher the CH_4 mole fraction
848 reading is (See Sect. S.9 in SI), but when several outlets are present at one location it is not
849 possible to uniquely determine the distance to the emission point, and also determine which
850 plume belongs to which outlet. Eq. 1 from Weller et al. (2019) only uses the maximum CH_4
851 enhancements above the 10% threshold from each pass. In their controlled release experiments
852 the average distance between the leak and measurement was 15.75 m. Analysis of our results
853 (Table S4, Sect S.5 in SI) shows that higher maximum concentrations are encountered more
854 often when the distances of the transect to the leak location are small. For example, at HH002
855 the transect was very close to the main emission point, which likely leads to the substantially
856 higher emission rate estimate derived from the mobile method (4.9 L min^{-1}) compared to the
857 tracer method (0.22 L min^{-1}). On the other hand, at HH011 the mobile method underestimates
858 the emission rate (See Sect. 3.3.1), as at this location the measurement distance to the leak was
859 larger than reference distance of 15.75 m applied by Weller et al. (2019). This suggests that to
860 reduce the quantification error for individual leak locations, distance should also be included
861 in an improved transfer equation.

862 The effect of neglecting or retaining the transects with enhancement maxima below the 10%
863 threshold was quantitatively investigated for 5 locations where the tracer team conducted
864 mobile measurements (See Sect. S.10 in SI). These measurements were evaluated as
865 “controlled release” experiments for C_2H_2 , because the actual C_2H_2 release rate is known, and
866 measurements were made in mobile mode. The standard mobile quantification algorithm with
867 the 10% threshold yields emission estimates that are in relatively good agreement with the
868 released quantities, whereas the estimates are biased considerably low when measurements



869 with maxima below the threshold are retained. This supports the use of the original method,
870 which removes transects with an improper realization of the plume. Relating to section 4.5, it
871 must be noted, however that in these measurements the distances of the C_2H_2 maxima to the
872 release points were between 30 to 45 m, thus larger than the normal distance of mobile CH_4
873 measurement to the emission outlets (from few meters up to 30 m).
874

875 **4.3.2 Tracer method**

876 The tracer method is more labor intensive than the mobile method. However, the strength of
877 the method is the application of a tracer gas providing the plume dilution and avoiding the use
878 of atmospheric dispersion models and weather information. If the tracer release location does
879 not reflect the sum of all the outlet emissions at a gas leak location, or misses some of the
880 outlets, then the total emission quantification from the gas leaks will be underestimated. An
881 example of such a case is site HH011 in this study where the leak location in the gas pipeline
882 (after quantification; see Fig. 1) was found to be located about 60 m upwind the targeted
883 emission outlet. During tracer quantification, an additional CH_4 plume (not defined by the
884 tracer gas) was observed indicating more than one emission outlet (Fig. 4). The confirmation
885 for this is the finding of gas leak location by the carpet method. The emission rate of the
886 targeted emission source (the vent and the drain) is thus not representing the combined
887 emission from the gas leak in the pipeline located 60 m upwind the emission source. Further
888 surface screening and leak detection would have been needed to identify and quantify all
889 emission outlets.
890

891 **4.3.3 Suction method**

892 The suction method is the most labor-intensive quantification method. Following a strict, safety
893 first, protocol the gas utilities fix leaks in the A1 safety category immediately upon detection
894 and A2 leaks within a week. Given logistical constraints, the suction method therefore mainly
895 or exclusively quantifies B or C leaks (50% of confirmed gas leak location in this study). We
896 investigated whether such a site selection bias could lead to a bias in the average quantified
897 emission rate in the inventory report. In this study, we observed that the leaks detected from
898 the mobile methods were mostly in the A1 and A2 category and the biggest emitters (based on
899 the mobile and tracer release measurements) had soil CH_4 accumulation of a magnitude that
900 prevented successful application of the suction method. Further research is needed to identify
901 the physical mechanism(s) to explain the observed correlation between A1 and A2 leaks and
902 high emission rates. As a hypothesis, the presence of soil cavities associated with leak category
903 A1 may result in higher permeability, i.e. lower underground resistance, which then leads to
904 higher emission rate for the same pipeline hole size compared to locations with no cavity.
905 The suction method was intended to be deployed right before the repair actions. For some of
906 these locations, the suction method was in operation for more than 10 hours, but due to the high
907 soil CH_4 accumulation, the measurements were stopped and labeled as incomplete in this study.
908 For the other locations with high soil CH_4 accumulation, the suction method was not attempted,
909 given the expectation (based on experience at the incomplete locations) that completion of
910 measurements for leak rate quantification at those locations was unlikely.
911

912 **4.3.4 Hole method**

913 Based on the leak size, pipeline depth and overpressure, the average emission rate was
914 estimated at 40 L min^{-1} ($n = 5$). We note that these estimated should be regarded as upper limits
915 since flow restrictions outside the pipe are not included. The emission range of individual gas
916 leaks based on the hole method is between 19 to 150 L min^{-1} for 1 cm^2 to 15 cm^2 hole sizes
917 respectively, larger than any of the measurement-based quantification methods. This method
918 requires information about the overpressure of the gas pipeline, depth of buried pipeline and



919 size of a leak and it does not include the information about soil properties, which can impact
920 the emission rate.

921

922 **4.3.5 Intercomparison of methods**

923 In this study, a reliable quantitative intercomparison of the three methods (mobile, tracer and
924 suction methods) was attempted. A complete comparison of all three methods was possible at
925 only one out of 20 locations (18 confirmed gas leak locations) because of the long time (>8-10
926 hrs) needed for full equilibrium of the suction method, whereby emission rates for 7 out of the
927 8 leaks quantified by the suction method were reported as maxima rather than absolute values
928 (Table 1). At these 7 locations the emission was thus overestimated.

929 In total, the average CH₄ emissions from natural gas pipeline leaks for the same locations where
930 we have quantifications from mobile and tracer methods (n = 13) are 2.8 and 1.2 L min⁻¹
931 respectively. The suction method could only be completed at one location. The average
932 emission rate reported for all the locations from the suction method (high bias due to
933 incomplete measurement) is 1.2 L min⁻¹ (n = 8).

934 The higher emission rates derived with the mobile method are in qualitative agreement with
935 previous studies. Weller et al. (2018) compared quantifications from the mobile measurements
936 described in von Fischer et al. (2017) with the tracer method and surface enclosure method in
937 four US cities. They reported that mobile measurement estimates were ≈ 2.3 L min⁻¹ greater
938 than the tracer method mean estimates of ≈ 3.2 L min⁻¹ (n = 59). This was attributed to the
939 overestimation of small leaks (< 2.4 L min⁻¹) in the mobile measurements method, which we
940 have also discussed above for our dataset. In addition, performance of only a few transects at
941 individual locations also lead to systematically high biased emission rate estimates for higher
942 emission rates (Luetschwager et al., 2021). Indeed, at the locations where we only have one
943 transects with CH₄ enhancements above the 10% threshold, there is an overestimation from
944 mobile method compared to the tracer method. For example, at HH001 (n=1), HH015 (n=1)
945 and HH100 (n=1) the mobile method estimated emissions of a factor 4 higher in comparison
946 to the tracer method. The analysis of Luetschwager (2019) clearly shows that this high bias is
947 reduced when numerous transects are performed. Therefore, we carried out multiple transects
948 to reduce this systematic bias. We note that there are also large differences between the mobile
949 and tracer methods, e.g. HH002 and HH006. We suspect that the very short gas leak location
950 distance to the mobile driving transects can explain partially the difference. Moreover,
951 existence of another leak in the category of A1 at the HH006 location which had to be fixed
952 prior to the tracer method could explain the difference in emission rate magnitude at this
953 location. Nevertheless, the limited number of transects and the 10% threshold can contribute
954 to an overestimation of the average leak rate with the mobile method at an individual location.
955 At the same time, however, the mobile method fails to detect leaks entirely when the leak outlet
956 is located downwind of the mobile van. The fact that the mobile method misses downwind
957 emissions constitutes a method specific factor towards biasing city-wide emissions low, which
958 qualitatively counteracts the high bias above.

959

960 **4.4 Possible suction method sampling bias with implications for emission inventories**

961 The national inventory for CH₄ leakage from the gas distribution network in Germany is based
962 on measurements with the suction technique (Umweltbundesamt, 2021). An ongoing project is
963 underway to refine these emission estimates (MEEM, 2022). The utilities choose leak locations
964 for application of the suction method where there are no safety concerns and/or immediate leak
965 closure is compulsory. This implies that this method is not applied at locations of the A1
966 category, which demand immediate repair (P. 27 in GERG, 2018). Due to logistic constraints
967 and the time-consuming nature of the suction measurements, they are likely also not (or rarely)
968 applied at locations in the A2 category, which require repair within a week. Thus, suction



969 measurements have a location sampling bias towards leaks in the B and C category. This is
970 supported by the fact that the leak locations that were contributed by the LDC to the
971 intercomparison campaign were locations in the B and C category. This study investigated
972 whether this location sampling bias could result in an emission rate bias, which could contribute
973 to the fact that the suction method did not report leaks with emission rates as high as they have
974 been reported by the mobile method in this study or during previous measurements in the same
975 city (Maazallahi et al., 2020).

976 In this study, emission rates from A1 and A2 category leaks were larger compared to those
977 from B and C category leaks (Figure 6). The emission rate differences vary by measurement
978 method: a factor 2 for the mobile method ($n = 9$ for A1&A2, $n = 4$ for B&C), a factor 11 for
979 the tracer method ($n = 8$ for A1&A2, $n = 8$ for B&C) and a factor 1.6 for the suction method
980 ($n=3$ for A1&A2, $n = 5$ B&C). For the mobile method, there is a clear separation between the
981 A1&A2 versus the B&C categories. The highest emission estimate for the B&C group
982 (HH010) is similar to the lowest emission rate estimate for the A1&A2 group (HH014).
983 Furthermore, HH011 in the A1 category was very likely biased low because of the wrongly
984 assumed leak location.

985 For the tracer method, the difference between the two groups is largest, an order of magnitude,
986 and we know that emissions are underestimated at least at one location of the A1 category
987 (HH011). The uncertainty of the tracer method is much smaller than the difference between the
988 two groups. The tracer method also illustrates that 4 of the 5 leaks that were contributed by the
989 LDC to the intercomparison campaign were extremely small. If these would be representative
990 for locations where the suction method is usually applied, it would indeed indicate a severe
991 emission rate bias for the suction method, not because the measurements themselves are biased,
992 but because locations with low emission rates are targeted with this method. In the
993 intercomparison campaign, we attempted to apply the suction method also at locations of the
994 A categories, but at 8 out of 9 locations from the A category, the suction measurements could
995 not be applied for safety reasons, or suction could not be completed, because of the widespread
996 subsurface accumulation (Table 2). At the other A location (HH014), the suction method could
997 not be applied as the ground had been already opened for the repair.

998

999 5 Conclusion

1000

1001 In summer 2020, we compared three gas leak rate quantification methods, namely the mobile,
1002 tracer, and suction methods, in Hamburg, Germany. While the mobile and tracer methods have
1003 been evaluated previously, this is the first peer-reviewed study that includes the suction
1004 method.

1005 The mobile method can cover large areas in a short time, but some of the smaller leaks (< 0.5
1006 $L \text{ min}^{-1}$) are not identified as a gas leak location due to the 10% enhancement threshold in the
1007 standard mobile quantification algorithm. While the mobile method quantification algorithm is
1008 designed to accurately report city-level total gas distribution leak rates (i.e., considering a large
1009 sample size), it has large (known) uncertainties for individual leaks. The tracer method has a
1010 smaller uncertainty, but it is labor intensive in comparison to the mobile method. On average,
1011 CH_4 emissions from natural gas pipeline leaks were higher from mobile quantifications in
1012 comparison to tracer quantifications. For many locations, we encountered several outlets and
1013 with widespread underground gas accumulations. At one location, after deployment of the
1014 mobile and the tracer quantification and during the repair actions, it was found out that the
1015 actual leak in the gas pipeline was located ≈ 60 m away from the identified emission outlet
1016 indicating significant underground gas migration. It is possible that this leak had several



1017 emission outlets that were not identified and the emission quantified from the single outlet is
1018 thus not representative for the whole emission from this leak.
1019 The suction method has a low reported uncertainty, but it is even more labor and time intensive
1020 than the tracer method. Due to the time and effort needed to plan and execute the measurements,
1021 the suction method is likely never applied in routine operation at A1 or A2 safety category
1022 leaks that mandate immediate or near-time repair. In our study, it was also not feasible to apply
1023 the suction method at locations with large subsurface CH₄ accumulations. Our results thus
1024 indicate a systematic difference between A1 and A2 (high emissions) versus B and C (low
1025 emissions) category locations, and generally larger emission rates are inferred with the mobile
1026 and tracer methods for sites with widespread subsurface accumulation.
1027 This study did not allow a direct, quantitative comparison of emission rates estimated with all
1028 three different methods because of the inability to quantify the same leak locations with all
1029 methods. However, this inability illuminates the importance of site selection for deriving
1030 representative emission factors based on empirical measurements. Specifically, the results
1031 suggest that a significant emission rate bias could exist for measurements that are carried out
1032 with the suction method. Our results therefore stipulate that representative site selection
1033 includes sampling at all leak safety categories (GERG, 2020). Otherwise, this could lead to a
1034 sampling and emission rate bias in the national inventory of gas leak CH₄ emission in Germany.
1035

1036 **Authors contributions:** TR, HM and SS conceived and designed the study. TR coordinated
1037 the campaign in collaboration with DBI, Technical University of Denmark (DTU),
1038 Environmental Defense Fund (EDF), E.On and Gasnetz Hamburg (GNH) teams. HM carried
1039 out the mobile measurements, emission outlet attribution, performed the analyses of mobile
1040 data and collectively with TR analyzed the intercomparison results. AD, CS and AMF
1041 performed the tracer method and reported the emission rates from the tracer dataset.
1042 HDvdG and TR made instruments and equipment available for the mobile method and CS
1043 provided those for the tracer method. HM wrote the paper, and all co-authors supported the
1044 interpretation of the results and contributed to improving the paper.
1045

1046 **Competing interests:** The authors declare that they have no conflict of interest.
1047

1048 Acknowledgement

1049 This study was carried out with the financial support from the Environmental Defense Fund.
1050 Extra financial supports were provided by the H2020 Marie Skłodowska-Curie actions through
1051 Methane goes Mobile – Measurements and Modelling project (MEMO²; [https://h2020-
1052 memo2.eu/](https://h2020-memo2.eu/), last access: 20 April 2022), grant number 722479. In this study, Robertson
1053 Foundation supported contribution of Stefan Schwietzke. We appreciate efforts from
1054 Luise Westphal, Michael Dammann, Ralf Luy, Christian Feickert, Volker Krell, Turhan Ulas,
1055 Dieter Bruhns and Sönke Graumann, from GasNetz Hamburg GmbH who facilitated this study
1056 by hosting the teams, arranging and applying the carpet method leak detection and confirmation
1057 procedures, making information on gas leaks and pipelines available for the data analysis and
1058 applying leak repair protocols. We extend our appreciation to Andre Lennartz, Stefan Gollanek
1059 and Dieter Wolf from E.On-for their contribution in the planning of the campaign, deploying
1060 the suction method at the locations, and exchanging their knowledge and experiences from
1061 their previous campaigns. We thank the team from DBI Gas and Environmental
1062 Technologies GmbH Leipzig (DBI GUT Leipzig) including Charlotte Große, who contributed
1063 in providing information for structuring the campaign planning.
1064
1065



Reference:

- 1066
1067 Alvarez, R. A., Pacala, S. W., Winebrake, J. J., Chameides, W. L., Hamburg, S. P.: Greater
1068 focus needed on methane leakage from natural gas infrastructure, *PNAS*, 109 (17)
1069 6435-6440, <https://doi.org/10.1073/pnas.1202407109>, 2012.
- 1070 Ars, S., Vogel, F., Arrowsmith, C., Heerah, S., Knuckey, E., Lavoie, J., Lee, C., Mostafavi Pak,
1071 N., Phillips, J. L., and Wunch, D., Investigation of the Spatial Distribution of Methane
1072 Sources in the Greater Toronto Area Using Mobile Gas Monitoring Systems, *Environ.*
1073 *Sci. Technol.*, 54, 24, 15671–15679, <https://doi.org/10.1021/acs.est.0c05386>, 2020.
- 1074 Allwine G., Lamb B., Westberg H., Application of Atmospheric Tracer Techniques for
1075 Determining Biogenic Hydrocarbon Fluxes from an Oak Forest. In: Hutchison B.A.,
1076 Hicks B.B. (eds) *The Forest-Atmosphere Interaction*. Springer, Dordrecht.
1077 https://doi.org/10.1007/978-94-009-5305-5_23, 1985.
- 1078 Arnaldos, J., Casal, J., Montiel, H., Sánchez-Carricondo, M., Vilchez, J.A., Design of a
1079 computer tool for the evaluation of the consequences of accidental natural gas releases
1080 in distribution pipes, *Journal of Loss Prevention in the Process Industries*,
1081 [https://doi.org/10.1016/S0950-4230\(97\)00041-7](https://doi.org/10.1016/S0950-4230(97)00041-7), 1998.
- 1082 Bousquet, P., Ciais, P., Miller, J. B., Dlugokencky, E. J., Hauglustaine, D. A., Prigent, C., Van
1083 der Werf, G. R., Peylin, P., Brunke, E. G., Carouge, C., Langenfelds, R. L., Lathière,
1084 J., Papa, F., Ramonet, M., Schmidt, M., Steele, L. P., Tyler, S. C., White, J.,
1085 Contribution of anthropogenic and natural sources to atmospheric methane variability.
1086 *Nature.*; 443(7110):439-43. <https://doi.org/10.1038/nature05132>, 2006.
- 1087 Brandt, A. R., Heath, G. A., and Cooley, D., Methane Leaks from Natural Gas Systems Follow
1088 Extreme Distributions, *Environmental Science & Technology*, 50 (22), 12512-12520,
1089 <https://doi.org/10.1021/acs.est.6b04303>, 2016
- 1090 Cho, Y., Ulrich, B. A., Zimmerle, D. J., Smits, K. M., Estimating natural gas emissions from
1091 underground pipelines using surface concentration measurements, *Environmental*
1092 *Pollution*, <https://doi.org/10.1016/j.envpol.2020.115514>, 2020.
- 1093 Defratyka, S. M., Paris, J. D., Yver-Kwok, C., Fernandez, J. M., Korben, P., and Bousquet, P.,
1094 *Environmental Science & Technology Article ASAP*,
1095 <https://doi.org/10.1021/acs.est.1c00859>, 2021.
- 1096 Delre, A., Greenhouse gas emissions from wastewater treatment plants: measurements and
1097 carbon footprint assessment, Ph.D. Thesis, Department of Environmental Engineering,
1098 Technical University of Denmark (DTU), Copenhagen, Available at:
1099 [https://orbit.dtu.dk/en/publications/greenhouse-gas-emissions-from-wastewater-](https://orbit.dtu.dk/en/publications/greenhouse-gas-emissions-from-wastewater-treatment-plants-measure)
1100 [treatment-plants-measure](https://orbit.dtu.dk/en/publications/greenhouse-gas-emissions-from-wastewater-treatment-plants-measure) (Last Accessed: 15 June 2021), 2018.
- 1101 DVGW: High-performing infrastructure, (2022). [online] Available from
1102 <https://www.dvgw.de/english-pages/topics/safety-and-security/technical-safety-gas>,
1103 (Last Accessed: 25 January 2022)
- 1104 DVGW: Technische Regel-Arbeitsblatt; DVGW G465-1 (A) (2019). [online] Available from:
1105 https://shop.wvgw.de/var/assets/leseprobe/510544_lp_G_465-1_2019_05.pdf. (Last
1106 Accessed: 15 December 2021)
- 1107 Ebrahimi-Moghadam, A., Farzaneh-Gord, M., Arabkoohsar, A., Jabari Moghadam, A., CFD
1108 analysis of natural gas emission from damaged pipelines: Correlation development for
1109 leakage estimation, *Cleaner Production*, <https://doi.org/10.1016/j.jclepro.2018.07.127>,
1110 2018.
- 1111 EC: EU strategy to reduce methane emissions available at: [https://eur-lex.europa.eu/legal-](https://eur-lex.europa.eu/legal-content/EN/TXT/?uri=CELEX%3A52020DC0663&qid=1644853088591)
1112 [content/EN/TXT/?uri=CELEX%3A52020DC0663&qid=1644853088591](https://eur-lex.europa.eu/legal-content/EN/TXT/?uri=CELEX%3A52020DC0663&qid=1644853088591), (last
1113 access: 28 March 2022), 2020



- 1114 EIA, Carbon Dioxide Emissions Coefficients, available at:
1115 https://www.eia.gov/environment/emissions/co2_vol_mass.php, (last access:
1116 28 March 2022), 2021.
- 1117 EPA, Methane emissions from the natural gas industry: underground pipelines,
1118 https://www.epa.gov/sites/production/files/2016-08/documents/9_underground.pdf,
1119 1996.
- 1120 Fernandez, J. M., Maazallahi, H., France, J. L., Menoud, M., Corbu, M., Ardelean, M., Calcan,
1121 A., Townsend-Small, A., van der Veen, C., Fisher, R. E., Lowry, D., Nisbet, E.G.,
1122 Röckmann, T.: Street-level methane emissions of Bucharest, Romania and the
1123 dominance of urban wastewater., *Atmospheric Environment: X*, 13, 2590-1621,
1124 100153, <https://doi.org/10.1016/j.aeaoa.2022.100153>, 2022.
- 1125 Fredenslund, A.M., Scheutz, C., Kjeldsen, P.: Tracer method to measure landfill gas emissions
1126 from leachate collection systems, *Waste Management*, 30, 2146-2152,
1127 <https://doi.org/10.1016/j.wasman.2010.03.013>, 2010
- 1128 Fredenslund, A. M., Rees-White, T. C., Beaven, R. P., Delre, A., Finlayson, A., Helmore, J.,
1129 Allen, G., Scheutz, C.: Validation and error assessment of the mobile tracer gas
1130 dispersion method for measurement of fugitive emissions from area sources, *Waste
1131 Management*, 83, 68-78, <https://doi.org/10.1016/j.wasman.2018.10.036>, 2019.
- 1132 Federal Environment Agency: National Inventory Report for the German Greenhouse Gas
1133 Inventory 1990 – 2018, available at: <https://unfccc.int/documents/226313> (last access:
1134 30 March 2022), 2020.
- 1135 GERG, Methane emission estimation method for the gas distribution grid (2018). [online]
1136 Available from: [https://www.gerg.eu/wp-
1137 content/uploads/2020/04/MEEM_Final_report.pdf](https://www.gerg.eu/wp-content/uploads/2020/04/MEEM_Final_report.pdf). (Last Accessed: 25 January 2022)
- 1138 GERG, Methane Emission Estimation Method for the Gas Distribution Grid (MEEM) (2020).
1139 [online], Available from: [https://www.gerg.eu/wp-
1140 content/uploads/2020/04/MEEM_Final_report.pdf](https://www.gerg.eu/wp-content/uploads/2020/04/MEEM_Final_report.pdf). (Last Accessed: 09 February 2022)
- 1141 Hendrick, M. F., Ackle, R., Sanaie-Movahed, B., Tang, X., Phillips, N. G., Fugitive methane
1142 emissions from leak-prone natural gas distribution infrastructure in urban
1143 environments, *Environmental Pollution*, <https://doi.org/10.1016/j.envpol.2016.01.094>,
1144 2016.
- 1145 Hou, Q., Yang, D., Li, X., Xiao, G. and Ho, S. C. M., Modified Leakage Rate Calculation
1146 Models of Natural Gas Pipelines, *Mathematical Problems in Engineering*,
1147 <https://doi.org/10.1155/2020/6673107>, 2020.
- 1148 Jackson, R. B., Saunio, M., Bousquet, P., Canadell, J. G., Poulter, B., Stavert, A. R.,
1149 Bergamaschi, P., Niwa, Y., Segers, A. and Tsuruta, A., Increasing anthropogenic
1150 methane emissions arise equally from agricultural and fossil fuel sources,
1151 *Environmental Research Letters*, 15, 071002, [https://doi.org/10.1088/1748-
1152 9326/ab9ed2](https://doi.org/10.1088/1748-9326/ab9ed2), 2020.
- 1153 Jackson, R. B., Down, A., Phillips, N. G., Ackley, R. C., Cook, C. W., Plata, D. L., and Zhao,
1154 K., Natural Gas Pipeline Leaks Across Washington, DC, *Environ. Sci. Technol.*, 48, 3,
1155 2051–2058, <https://doi.org/10.1021/es404474x>, 2014.
- 1156 Kirchgessner, D. A., Lott R. A., Cowgill, R.M., Harrison, M. R., Shires, T. M., Estimate of
1157 methane emissions from the U.S. natural gas industry, *Chemosphere*,
1158 [https://doi.org/10.1016/S0045-6535\(97\)00236-1](https://doi.org/10.1016/S0045-6535(97)00236-1), 1997.
- 1159 Keyes, T., Ridge G., Klein, M., Phillips, N., Ackley, R., Yang Y., An enhanced procedure for
1160 urban mobile methane leak detection. *Heliyon*. 9; 6 (10):e04876.
1161 <https://doi.org/10.1016/j.heliyon.2020.e04876>, 2020.
- 1162 Lamb, B. K., McManus, J. B., Shorter, J. H., Kolb, C. E., Mosher, B., Harriss, R. C., Allwine,
1163 E., Blaha, D., Howard, T., Guenther, A., Lott, R. A., Siverson, R., Westburg, H., and



- 1164 Zimmerman, P., Development of atmospheric tracer methods to measure methane
1165 emissions from natural gas facilities and urban areas, *Environmental Science &*
1166 *Technology* 29 (6), 1468-1479 <https://doi.org/10.1021/es00006a007>, 1995.
- 1167 Lamb, B. K., Edburg, S. L., Ferrara, T. W., Howard, T., Harrison, M. R., Kolb, C. E.,
1168 Townsend-Small, A., Dyck, W., Possolo, A., and Whetstone, J. R., *Environmental*
1169 *Science & Technology* 49 (8), 5161-5169 <https://doi.org/10.1021/es505116p>, 2015.
- 1170 Luetschwager, E., von Fischer, J. C., Weller, Z. D., Characterizing detection probabilities of
1171 advanced mobile leak surveys: Implications for sampling effort and leak size estimation
1172 in natural gas distribution systems. *Elementa: Science of the Anthropocene*; 9 (1):
1173 00143. <https://doi.org/10.1525/elementa.2020.00143>, 2021.
- 1174 Liu, C., Liao, Y., Liang, J., Cui, Z., Li, Y., Quantifying methane release and dispersion
1175 estimations for buried natural gas pipeline leakages, *Process Safety and Environmental*
1176 *Protection*, <https://doi.org/10.1016/j.psep.2020.11.031>, 2021.
- 1177 Maazallahi, H., Fernandez, J. M., Menoud, M., Zavala-Araiza, D., Weller, Z. D., Schwietzke,
1178 S., von Fischer, J. C., Denier van der Gon, H., and Röckmann, T.: Methane mapping,
1179 emission quantification, and attribution in two European cities: Utrecht (NL) and
1180 Hamburg (DE), *Atmos. Chem. Phys.*, 20, 14717–14740, <https://doi.org/10.5194/acp-20-14717-2020>, 2020.
- 1182 Mahgerefteh, H., Oke, A., Atti, O., Modelling outflow following rupture in pipeline networks,
1183 *Chemical Engineering Science*, <https://doi.org/10.1016/j.ces.2005.10.013>, 2006.
- 1184 MEEM, Analysing the Methods for Determination of Methane Emissions of the Gas
1185 Distribution Grid (2022). [online] Available from [https://www.dbi-](https://www.dbi-gut.de/emissions.html)
1186 [gut.de/emissions.html](https://www.dbi-gut.de/emissions.html). (Last Accessed: 25 January 2022)
- 1187 Moloudi, R., Abolfazli Esfahani, J., Modeling of gas release following pipeline rupture:
1188 Proposing non-dimensional correlation, *Journal of Loss Prevention in the Process*
1189 *Industries*, <https://doi.org/10.1016/j.jlp.2014.09.003>, 2014.
- 1190 Mønster, J. G., Samuelsson, J., Kjeldsen, P., Rella, C. W., Scheutz, C., Quantifying methane
1191 emission from fugitive sources by combining tracer release and downwind
1192 measurements – A sensitivity analysis based on multiple field surveys, *Waste*
1193 *Management*, 34, 1416-1428, <https://doi.org/10.1016/j.wasman.2014.03.025>, 2014.
- 1194 Myhre, G., Shindell, D., Bréon, F. M., Collins, W., Fuglestvedt, J., Huang, J., Koch, D.,
1195 Lamarque, J. F., Lee, D., Mendoza, B., Nakajima, T., Robock, A., Stephens, G.,
1196 Takemura, T., and Zhan, H.: Anthropogenic and Natural Radiative Forcing, in:
1197 *Climate Change 2013: The Physical Science Basis*, Contribution of Working Group I
1198 to the Fifth Assessment Report of the Intergovernmental Panel on Climate Change,
1199 Cambridge, UK and New York, NY, USA, available at:
1200 https://www.ipcc.ch/site/assets/uploads/2018/02/WG1AR5_Chapter08_FINAL.pdf,
1201 2013.
- 1202 Nisbet, E. G., Manning, M. R., Dlugokencky, E. J., Fisher, R. E., Lowry, D., Michel, S. E.,
1203 Myhre, C. L., Platt, S. M., Allen, G., Bousquet, P., Brownlow, R., Cain, M., France, J.
1204 L., Hermansen, O., Hossaini, R., Jones, A. E., Levin, I., Manning, A. C., Myhre, G.,
1205 Pyle, J. A., Vaughn, B. H., Warwick, N. J., White, J. W. C., Very strong atmospheric
1206 methane growth in the 4 Years 2014–2017: implications for the Paris agreement, *Global*
1207 *Biogeochemical Cycles*, 33, 318 – 342, <https://doi.org/10.1029/2018GB006009>, 2019.
- 1208 Okamoto, H., Gomi, Y., Empirical research on diffusion behavior of leaked gas in the ground,
1209 *Journal of Loss Prevention in the Process Industries*,
1210 <https://doi.org/10.1016/j.jlp.2011.01.007>, 2011.
- 1211 Phillips, N. G., Ackley, R., Crosson, E. R., Down, A., Hutyra, L. R., Bronfield, M., Karr, J.
1212 D., Zhao, K., Jackson, R. B., Mapping urban pipeline leaks: Methane leaks across



- 1213 Boston, Environmental Pollution, 173, 1-4,
1214 <https://doi.org/10.1016/j.envpol.2012.11.003>, 2013.
- 1215 Scheutz, C., Samuelsson, J., Fredenslund, A.M., Kjeldsen, P., Quantification of multiple
1216 methane emission sources at landfills using a double tracer technique, Waste
1217 Management, 31, 1009-1017, <https://doi.org/10.1016/j.wasman.2011.01.015>, 2011.
- 1218 Ulrich, B. A., Mitton, M., Lachenmeyer, E., Hecobian, A., Zimmerle, D., and Smits, K. M.,
1219 Natural Gas Emissions from Underground Pipelines and Implications for Leak
1220 Detection, Environmental Science & Technology Letters, 6 (7), 401-406,
1221 <https://doi.org/10.1021/acs.estlett.9b00291>, 2019.
- 1222 Umweltbundesamt, Berichterstattung unter der Klimarahmenkonvention der Vereinten
1223 Nationen und dem Kyoto-Protokoll 2021, [Online], Available from:
1224 https://www.umweltbundesamt.de/sites/default/files/medien/5750/publikationen/2021-05-19_cc_43-2021_nir_2021_1.pdf, (Last Accessed: 08 February 2022)
- 1225
1226 Von Fischer, J. C., Cooley, D., Chamberlain, S., Gaylord, A., Griebenow, C. J., Hamburg, S.
1227 P., Salo, J., Schumacher, R., Theobald, D., and Ham, J.: Rapid, Vehicle-Based
1228 Identification of Location and Magnitude of Urban Natural Gas Pipeline Leaks,
1229 Environ. Sci. Technol., 51, 4091–4099, <https://doi.org/10.1021/acs.est.6b06095>, 2017.
- 1230 Weller, Z. D., Roscioli, J. R., Daube, W. C., Lamb, B. K., Ferrara, T. W., Brewer, P. E., and
1231 von Fischer, J. C.: Vehicle-Based Methane Surveys for Finding Natural Gas Leaks and
1232 Estimating Their Size: Validation and Uncertainty, Environ. Sci. Technol., 52, 11922–
1233 11930, <https://doi.org/10.1021/acs.est.8b03135>, 2018.
- 1234 Weller, Z. D., Yang, D. K., and von Fischer, J. C.: An open source algorithm to detect natural
1235 gas leaks from mobile methane survey data, edited by: Mauder, M., PLoS One, 14,
1236 e0212287, <https://doi.org/10.1371/journal.pone.0212287>, 2019.
- 1237 Weller, Z. D., Hamburg, S. P., and von Fischer, J. C., A National Estimate of Methane Leakage
1238 from Pipeline Mains in Natural Gas Local Distribution Systems, Environmental
1239 Science & Technology, 54 (14), 8958-8967, <https://doi.org/10.1021/acs.est.0c00437>,
1240 2020
- 1241 Wiesner, S., Gröngröft, A., Ament, F. et al. Spatial and temporal variability of urban soil water
1242 dynamics observed by a soil monitoring network. J Soils Sediments 16, 2523–2537.
1243 <https://doi.org/10.1007/s11368-016-1385-6>, 2016
- 1244 Worden, J. R., Anthony Bloom, A., Pandey, S., Jiang, Z., Worden, H. M., Walker, T. W.,
1245 Houweling, S., Röckmann, T., , Reduced biomass burning emissions reconcile
1246 conflicting estimates of the post-2006 atmospheric methane budget, Nature
1247 Communications 8, 2227 <https://doi.org/10.1038/s41467-017-02246-0>, 2017
- 1248 Yan, Y., Dong, X., Li, J., Experimental study of methane diffusion in soil for an underground
1249 gas pipe leak, Journal of Natural Gas Science and Engineering,
1250 <https://doi.org/10.1016/j.jngse.2015.08.039>, 2015.
- 1251 Yuhua, D., Huilin, G., Jing'en, Z., Yaorong, F., Evaluation of gas release rate through holes in
1252 pipelines, Journal of Loss Prevention in the Process Industries,
1253 [https://doi.org/10.1016/S0950-4230\(02\)00041-4](https://doi.org/10.1016/S0950-4230(02)00041-4), 2002.
1254